the gene expression was much lower than that obtained with lipoplex. However, this was the maximal tolerated N/P ratio since a further increase to 15 was lethal for 6-h evaluation. In contrast, the linear PEI polyplex yielded similar levels to lipoplex at N/P ratios of 20 and 25 (Fig. 2D). The maximal tolerated N/P ratio of the linear PEI polyplex was 30.

Intravenously injected lipoplex induced the production of proinflammatory cytokines such as TNF-α, IFN-γ, and IL-12 (Whitmore et al., 1999; Sakurai et al., 2002). Among these cytokines, TNF-α is the primary source of toxicity because it induces septic shock in animals at high concentrations (Tan et al., 2002). Then, the response to an i.v. administration of a preparation of PEI polyplex varying in N/P ratio and the structure and molecular weight of PEI was investigated. After the injection, a significantly high TNF-α concentration was observed in serum (Fig. 3). The branched PEI was not lethal at an N/P ratio of up to 15 as of 3 h after the injection. After the i.v. injection of PEI polyplex, however, the TNF-α concentration was compatible with the control value (no treatment) and was significantly lower than that after the injection of lipoplex ($P < 0.01$). Moreover, this reduction in response was independent of the N/P ratio of the polyplex or structure and molecular weight of PEI (Fig. 3, A–D), although these factors could affect the gene expression in the lung and liver. When a linear PEI polyplex was prepared at an N/P ratio of 20, the efficacy of transfection increased without lethal toxicity. Accordingly, a linear PEI polyplex with an N/P ratio of 20 was selected for further investigation.

Effect of pDNA Dose and Time Course of PEI Polyplex on Cytokine Response. The transfection efficiency of the linear PEI polyplex was enhanced by the increasing of the pDNA dose (Fig. 4A). However, the TNF-α concentration obtained with PEI polyplex at a pDNA dose of 30, 50, and 80 μg was significantly lower than that obtained with lipoplex at a pDNA dose of 30 μg (Fig. 4B). To investigate the cytokine response in detail, serum levels of not only TNF-α but also IFN-γ and IL-12 were measured for 12 h (Fig. 5, A–C). These proinflammatory cytokines were significantly induced by the administration of lipoplex. This characteristic was consistent with the previous results about lipoplex (Whitmore et al., 1999; Sakurai et al., 2002). However, TNF-α, IFN-γ, and IL-12 concentrations were much lower after the injection of PEI polyplex than that of lipoplex (Fig. 5).

Serum ALT Activity Triggered by PEI Polyplex. To evaluate the toxicity in the liver, the serum ALT level was determined. Raising the dose of pDNA (30 and 50 μg) in lipoplex increased the serum ALT level, and 80 μg of pDNA was lethal (Fig. 6A). Increasing the dose of pDNA (30, 50, and 80 μg) in the linear PEI polyplex also increased the serum ALT level (Fig. 6B). When we checked the liver surface after abdominal operation, the damage of hepatic lobule was observed after mice administered the linear PEI_{25} polyplex at a pDNA dose of 50 and 80 μg.

Amount of Hepatic NFκB Activated by Linear PEI Polyplex. To investigate the mechanism of the cytokine response by linear PEI polyplex, the amount of activated NFκB was measured. After i.v. administration of lipoplex, significantly more activated NFκB was detected ($P < 0.05$). In contrast, the amount activated by the PEI polyplex was compatible with the control (no treatment group) and was significantly lower than that in response to lipoplex ($P < 0.05$) (Fig. 7).

Biodistribution of Linear PEI Polyplex. Biodistribution was examined to determine the difference in cytokine response to lipoplex versus the linear PEI polyplex (Fig. 8). [^{32}P] Linear PEI polyplex mostly accumulated in the liver after the i.v. administration, whereas [^{32}P] lipoplex accumulated in the lung. Blood concentration profiles of [^{32}P] linear PEI polyplex and [^{32}P] lipoplex did not differ.

Gene Expression Characteristics of Linear PEI Polyplex. Previous studies suggested that proinflammatory cytokines cause gene inactivation such as transient gene expres-

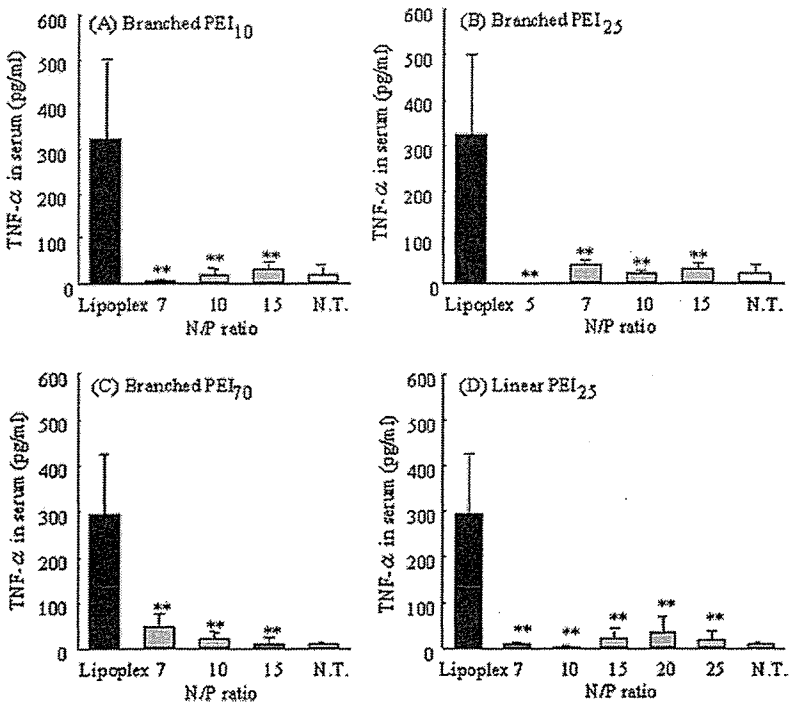

Fig. 3. Effect of N/P ratio of PEI polyplex and molecular weight of PEI on TNF-α release after the i.v. administration of branched and linear PEI polyplexes delivering 30 μg of pDNA per mouse. Branched PEI_{10} (A), PEI_{25} (B), and PEI_{70} (C), and linear PEI_{25} (D) were used to produce polyplexes with an N/P ratio of 7, 10, 15, or 20 and 25, respectively. Lipoplex had a −:+ of 1.0:3.1 and delivered 30 μg of pDNA per mouse. Mice were sacrificed at 3 h after the administration, and the concentration of TNF-α was measured. N.T., no treatment. Each value represents the mean + S.D. for at least three mice. **, statistically significant difference from the control group ($P < 0.01$).

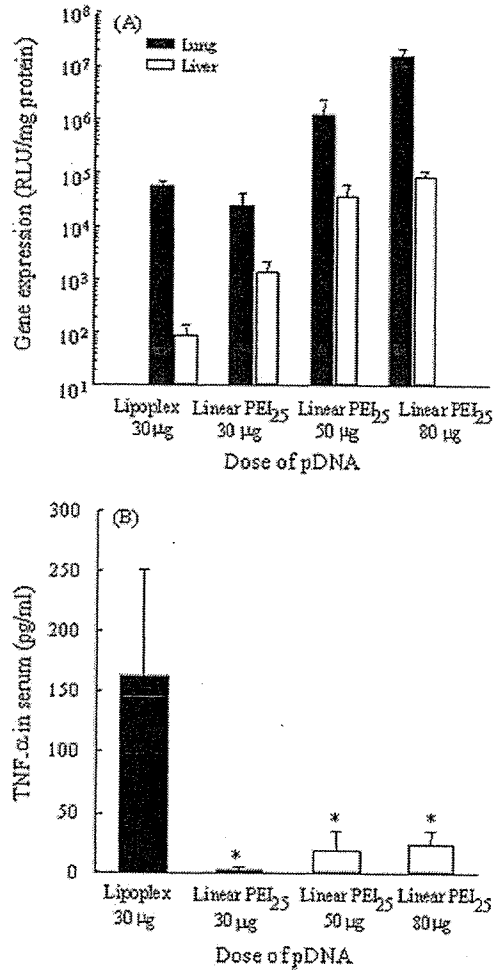

Fig. 4. Effect of the dose of pDNA on gene expression (A) and release of TNF-α (B) after the i.v. administration of linear PEI polyplex delivering 30, 50, and 80 μg of pDNA per mouse, respectively. Linear PEI polyplex was prepared at an N/P ratio of 20. Lipoplex had a −:+ of 1.0:3.1 and delivered 30 μg of pDNA per mouse. Mice were sacrificed at 6 h after administration, and levels of luciferase activity in the lung (filled bars) and liver (open bars) were measured. Mice also were sacrificed at 3 h after administration, and TNF-α concentrations were measured. *, statistically significant difference between the groups indicated ($P < 0.05$). Each value represents the mean + S.D. of at least three mice.

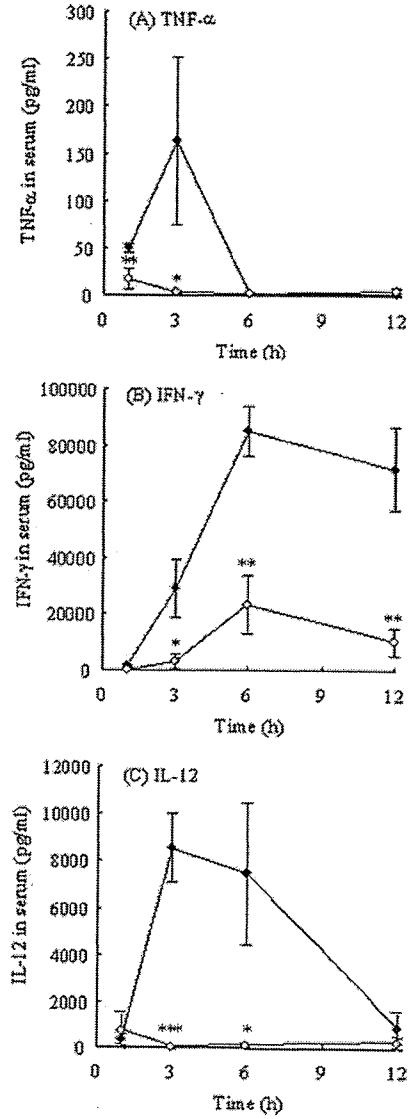

Fig. 5. Serum TNF-α (A), IFN-γ (B), and IL-12 (C) concentrations after the i.v. administration of linear PEI polyplex. Lipoplex (closed circles) was prepared with a −:+ of 1.0:3.1 and delivered 30 μg of pDNA per mouse. Linear PEI polyplex (open circles) was prepared at an N/P ratio of 20 with a pDNA dose of 30 μg per mouse. At the indicated time points after the administration of lipoplex or PEI polyplex, serum samples were collected from mice, and concentrations of TNF-α, IFN-γ, and IL-12 were measured. Each value represents the mean ± S.D. for at least three mice. Statistically significant difference from lipoplex (*, $P < 0.05$; **, $P < 0.01$; ***, $P < 0.001$).

sion on a single injection of lipoplex and a refractory period on repeated dosing (Li et al., 1999; Tan et al., 2001). To investigate whether the linear PEI polyplex provides long-term gene expression, its effect was compared with that of lipoplex at various time points. However, there was little difference in gene expression between linear PEI polyplex and lipoplex (Fig. 9).

Discussion

To clarify the relationship between gene expression and cytokine production in response to PEI polyplex, first, gene expression characteristics after the i.v. administration of the polyplex were evaluated based on the N/P ratio of PEI polyplex, the dose of pDNA, and the structure and molecular weight of PEI. After the i.v. administration in mice, the highest level of gene expression was observed in the lung. The gene expression characteristics were affected by the N/P ratio of polyplex and the structure and molecular weight of PEI (Fig. 2) as well as the dose of pDNA (Fig. 4A). These observations are consistent with previous reports (Goula et al., 1998; Bragonzi et al., 2000; Wightman et al., 2001; Zou et al., 2001). In this study, we selected DOTMA/cholesterol liposomes as cationic liposomes to prepare the lipoplex because of their high transfection efficacy in vivo (Song et al., 1997; Kawakami et al., 2000a; Sakurai et al., 2001). As shown in Fig. 2, the linear PEI polyplex induced the highest level of gene expression among the polyplexes under optimized conditions and was equal in efficacy to lipoplex. These observations are consistent with those of Bragonzi et al. (2000), who found that the gene expression efficacy of linear PEI polyplex was equal to lipoplex under optimal conditions.

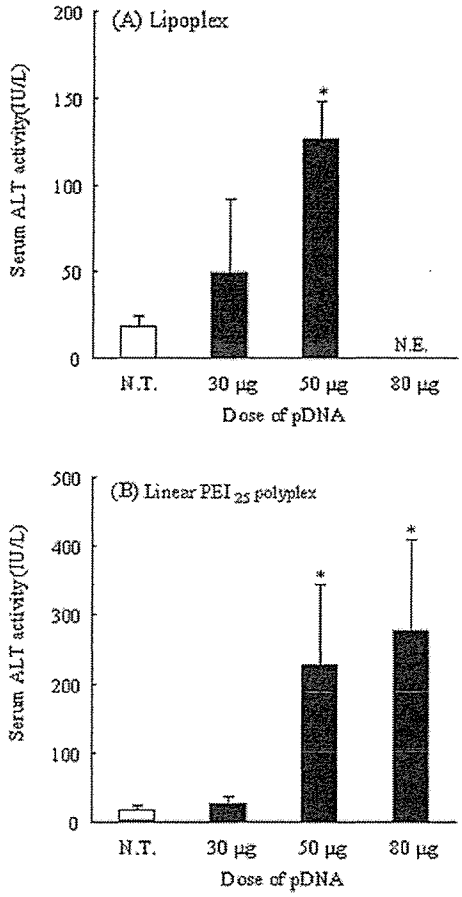

Fig. 6. Serum ALT activity after the i.v. administration of linear PEI polyplex. Lipoplexes were prepared with a −:+ of 1.0:3.1 and a pDNA dose of 30, 50, and 80 μg per mouse (A). Linear PEI polyplexes were prepared with a pDNA dose of 30, 50, and 80 μg per mouse (B). Mice were sacrificed at 24 h after the administration, and the ALT level in serum was measured. N.E., not evaluated. N.T., no treatment. *, statistically significant difference from untreated groups ($P < 0.05$). Each value represents the mean + S.D. for at least three mice.

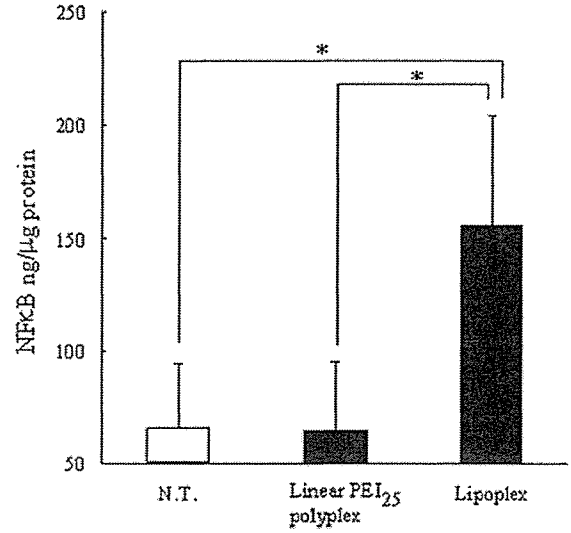

Fig. 7. Amount of activated NFκB in the liver after i.v. administration of linear PEI polyplex. Linear PEI polyplex was prepared at a pDNA dose of 30 μg per mouse. Lipoplex was prepared at −:+ of 1.0:3.1 and a pDNA dose of 30 μg per mouse. Mice were sacrificed at 3 h after the administration, and the amount of activated NFκB in the liver was measured. N.T., no treatment. *, statistically significant difference from the untreated group ($P < 0.05$). Each value represents the mean + S.D. for at least three mice.

Then, cytokine response characteristics after the i.v. administration of PEI polyplex were evaluated based on the N/P ratio of PEI polyplex, the dose of pDNA, and the structure and molecular weight of PEI. Interestingly, serum TNF-α levels were low irrespective of the N/P ratio of PEI polyplex and structure and molecular weight of PEI (Fig. 3) or the dose of pDNA (Fig. 4B), although these factors affected the transfection efficacy in vivo (Figs. 2 and 4A). These findings are partly supported by the report that the serum TNF-α level was much lower in mice administered linear PEI_{22} polyplex (N/P ratio, 6; pDNA dose, 25 μg/mouse) than those given lipoplex (Tan et al., 2001). To confirm whether this response is specific to TNF-α at 3 h, TNF-α, IFN-γ, and IL-12 concentrations were measured until 12 h; consequently, TNF-α, IFN-γ, and IL-12 concentrations by linear PEI polyplex were also much lower than that by lipoplex at various time points (Fig. 5). All of these results provide evidence that PEI polyplex hardly induced the production of proinflammatory cytokines irrespective of the N/P ratio of PEI polyplex, dose of pDNA, or structure and molecular weight of PEI, although these are important factors for transfection efficacy in vivo (Figs. 2 and 4A).

NFκB is a central regulator of inflammatory and immune responses (Barnes and Karin, 1997) and is crucial for the transcription of multiple proinflammatory molecules, including TNF-α, IL-1β, IL-2, IL-6, IL-8, IL-12, and IFN-β (Lenardo and Baltimore, 1989). To investigate further the production of cytokines in response to PEI polyplex, the amount of activated NFκB in liver was measured. As shown in Fig. 7, we demonstrated that the amount of NFκB activated by linear PEI polyplex was comparable with the control level (untreated group) and was significantly lower than that activated by lipoplex ($P < 0.05$). In contrast, the amount of hepatic NFκB activated by lipoplex was significantly enhanced. These results are well consistent with the concentrations of proinflammatory cytokines produced when lipoplex and linear PEI polyplex were administered (Fig. 5). Thus, these observations lead us to conclude that lower levels of proinflammatory cytokines are produced in response to PEI polyplex after i.v. administration.

The immunostimulatory response observed in mammalian cells has been shown to arise in part from the recognition of the unmethylated CpG dinucleotides present in bacterial DNA or pDNA. Yi et al. (1998) reported that the activation of leukocyte by CpG DNA might occur in association with the acidification of endosomes since chloroquine, which is an inhibitor of endosomal acidification, blocks CpG DNA-induced IκBα and IκBβ degradation and the subsequent activation of NFκB; consequently, the response to produce proinflammatory cytokines is reduced. Likewise, Yew et al. (2000) demonstrated that two such inhibitors, chloroquine and quinacrine, greatly reduced the production of IL-12 by mouse spleen cells in vitro and inhibited cytokine production in the lung by approximately 50% without affecting gene expression. It has been reported that the transfection efficiency of PEI polyplex is due to its capacity to buffer the endosome (proton sponge effect) (Boussif et al., 1995; Kichler et al., 2001; Akinc et al., 2005); therefore, such a property might

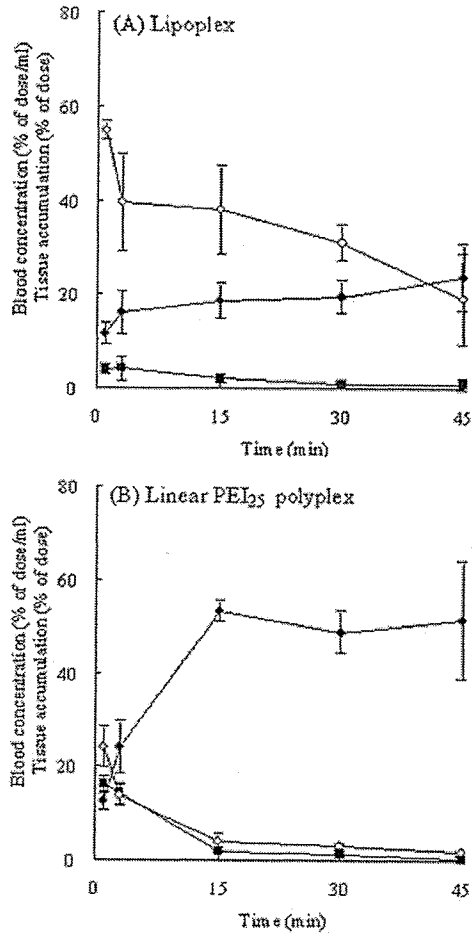

Fig. 8. Biodistribution after the i.v. administration of [^{32}P] linear PEI polyplex. Linear PEI polyplex was prepared at a pDNA dose of 30 μg per mouse. Lipoplex was prepared at −:+ of 1.0:3.1 at a pDNA dose of 30 μg per mouse. Blood (filled squares) was collected from the vena cava, liver (filled circles), and lung (open circles) at 1, 3, 15, 30, and 45 min, and levels of radioactivity in lung (A) and liver (B) were measured. Each value represents the mean ± S.D. for at least three mice.

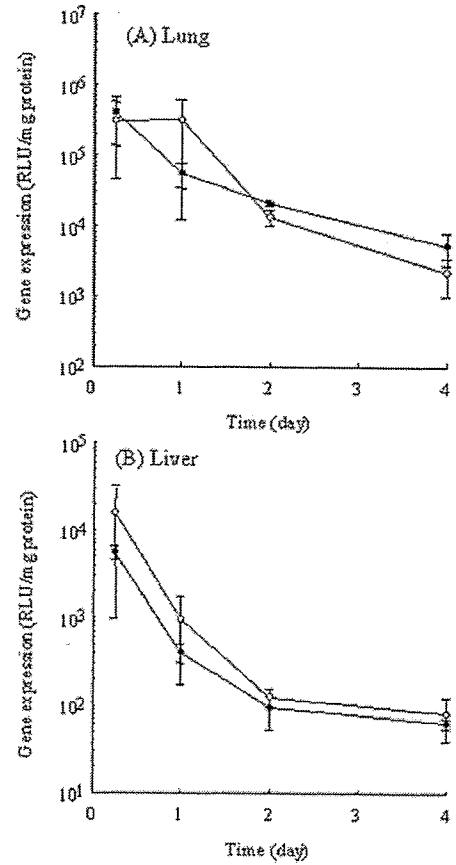

Fig. 9. Time course of gene expression in the lung (A) and liver (B) after the i.v. administration of linear PEI polyplex. Linear PEI polyplex (open circle) was prepared at a pDNA dose of 30 μg per mouse. Lipoplex (closed circle) was prepared at −:+ of 1.0:3.1 at a pDNA dose of 30 μg per mouse. At the indicated time point, mice were sacrificed, and luciferase activity was measured. Each value represents the mean ± S.D. for at least three mice.

abolish the pDNA (CpG DNA)-induced activation of NFκB (Fig. 7).

We previously investigated the distribution of lipoplex and demonstrated that when i.v. injected, it was predominantly taken up by Kupffer cells via the phagocytic process that is responsible for the production of proinflammatory cytokines (Sakurai et al., 2002). Taking this into consideration, we hypothesized that the hepatic uptake of PEI polyplex is less than that of lipoplex. However, the biodistribution study demonstrated that much more [^{32}P] linear PEI polyplex than [^{32}P] lipoplex accumulates in the liver (Fig. 8). These results suggested that the difference in the response induced by PEI polyplex and lipoplex could not explain their distribution.

As far as the pulmonary accumulation of lipoplex is concerned, we and other groups have reported that lipoplex-induced hemagglutination is an important factor in the localization of lipoplex to the lung (Sakurai et al., 2001; Fumoto et al., 2005). It should be considered that the hemagglutination is caused by electrostatic interaction between the erythrocytes and lipoplex. In the distribution study, the ζ potential of PEI polyplex (approximately 40 mV) (Fig. 1) was lower than that of lipoplex (approximately 60 mV), suggesting less electrostatic interaction between the erythrocytes and linear PEI polyplex. This hypothesis may be partly supported by the report that the aggregation of erythrocytes caused by linear PEI polyplex was minimal (Kircheis et al., 2001). Such ζ potential characteristics may reflect a more hepatic-selective distribution of the linear PEI polyplex (Fig. 8).

To evaluate hepatic damage, serum ALT activity was measured. As shown in Fig. 6A, raising the dose of pDNA in the lipoplex preparation increased the serum level of ALT. This finding regarding toxicity was consistent with the previous reports (Tousignant et al., 2000; Loisel et al., 2001). Recently, Tan et al. (2001) suggested that such hepatic damage was caused by the proinflammatory cytokines secreted when lipoplex was injected i.v. In this study, we demonstrated that PEI polyplex hardly induced the production of any proinflammatory cytokines (Figs. 3–5), but hepatic toxicity was observed (Fig. 6B). These observations provide evidence that the hepatic damage is not mediated by the proinflammatory cytokines, suggesting that the mechanisms behind the toxicity of lipoplex and linear PEI polyplex are different. Recently, Moghimi et al. (2005) reported PEI polyplex (branched and linear), by using calf thymus DNA, induced the cytotoxicity (necrosis and/or apoptosis) in several cultured human cell

lines. These results also suggested hepatic damage might be induced by PEI itself.

In this study, we examined the effect of the dose of pDNA in the PEI polyplex on hepatic damage. As shown in Fig. 6B, serum ALT activity at 30 μg of pDNA was compatible with the control (no treatment). However, at higher doses (50 and 80 μg), the serum ALT level increased, suggesting that i.v. injected PEI polyplex causes hepatic damage in a pDNA dose-dependent manner. These observations are consistent with those of Chollet et al. (2002), whose histological analysis revealed necrosis in the liver after the i.v. administration of a linear polyplex containing 100 μg of pDNA.

As shown in Fig. 6, lipoplex at pDNA dose of 80 μg was lethal. This observation corresponded with Hofland et al. (1997), who reported lipoplex at the pDNA dose of approximately 80 μg was the maximal tolerated dose in mice. It is expected that the hepatic toxicity between lipoplex and polyplex at pDNA dose of 80 μg is to the same extent since hepatic toxicity was nearly similar between lipoplex and PEI polyplex at pDNA dose of 30 and 50 μg (Fig. 6). Therefore, the lethal effect of lipoplex at pDNA dose of 80 μg might be explained by cytokine response, hematologic and serologic changes typified by leukopenia and thrombocytopenia (Tousignant et al., 2000).

Goula et al. (1998) reported that the branched PEI_{25} polyplex was lethal within a few minutes even when used at a low N/P ratio, although how it was prepared is not clear. As shown in Fig. 2, the maximal tolerated N/P ratio of branched PEI_{10}, PEI_{25}, and PEI_{70} was 10 since a further increase to 15 was lethal in 6 h. Thus, this observation is consistent with the report by Goula et al. (1998). Our results also suggested that the lethal toxicity of the branched PEI polyplex does not depend on the molecular weight of PEI.

In conclusion, the concentration of proinflammatory cytokines, such as TNF-α, produced were much lower when PEI polyplex rather than lipoplex was administered irrespective of the N/P ratio of the polyplex, dose of pDNA used, or structure and molecular weight of PEI, although these factors affected the transfection efficacy in vivo. We demonstrated that the amount of NFκB activated by the linear PEI polyplex was comparable with the control (untreated group) and was significantly lower than that when lipoplex was administered. Although the production of proinflammatory cytokines (TNF-α, IFN-γ, and IL-12) was reduced by the administration of the linear PEI polyplex, serum ALT levels were significantly enhanced by pDNA in a dose-dependent manner, suggesting that the hepatic damage is not induced by proinflammatory cytokines. This information will be valuable for the development of nonviral vectors for clinical applications.

References

Akinc A, Thomas M, Klibanov AM, and Langer R (2005) Exploring polyethylenimine-mediated DNA transfection and the proton sponge hypothesis. *J Gene Med* **7**:657–663.

Barnes PJ and Karin M (1997) Nuclear factor-κB: a pivotal transcription factor in chronic inflammatory diseases. *N Engl J Med* **336**:1066–1071.

Boletta A, Benigni A, Lutz J, Remuzzi G, Soria MR, and Monaco L (1997) Nonviral gene delivery to the rat kidney with polyethylenimine. *Hum Gene Ther* **8**:1243–1251.

Boussif O, Lezoualc HF, Zanta AM, Mergny DM, Scherman D, Demeneix B, and Behr JP (1995) A versatile vector for gene and oligonucleotide transfer into cells in culture and *in vivo*: polyethylenimine. *Proc Natl Acad Sci USA* **92**:7297–7301.

Bragonzi A, Dina G, Villa A, Calori G, Biffi A, Bordignon C, Assael BM, and Conese M (2000) Biodistribution and transgene expression with nonviral cationic vector/DNA complexes in the lungs. *Gene Ther* **7**:1753–1760.

Chollet P, Favrot MC, Hurbin A, and Coll JL (2002) Side-effects of a systemic injection of linear polyethylenimine-DNA complexes. *J Gene Med* **4**:84–91.

David PS, Shalin N, Shannon JB, David AH, and Katryn JS (2000) Phosphorothioate backbone modification modulates macrophage activation by CpG DNA. *J Immunol* **165**:4165–4173.

Freimark BD, Blezinger HP, Florack VJ, Nordstrom JL, Long SD, Deshpande DS, Nochumson S, and Petrak KL (1998) Cationic lipids enhance cytokine and cell influx levels in the lung following administration of plasmid: cationic lipid complexes. *J Immunol* **160**:4580–4586.

Fumoto S, Kawakami S, Shigeta K, Higuchi Y, Yamashita F, and Hashida M (2005) Interaction with blood components plays a crucial role in asialoglycoprotein receptor-mediated in vivo gene transfer by galactosylated lipoplex. *J Pharmacol Exp Ther* **315**:484–493.

Goula D, Benoist C, Mantero S, Merlo G, Levi G, and Demeneix BA (1998) Polyethylenimine-based intravenous delivery of transgenes to mouse lung. *Gene Ther* **5**:1291–1295.

Hofland HEJ, Nagy D, Liu JJ, Spratt K, Lee YL, Danos O, and Sullivan SM (1997) In vivo Gene transfer by intravenous administration of stable cationic lipid/DNA complex. *Pharm Res (N Y)* **14**:742–749.

Kawakami S, Fumoto S, Nishikawa M, Yamashita F, and Hashida M (2000a) In vivo gene delivery to the liver using novel galactosylated cationic liposomes. *Pharm Res (N Y)* **17**:306–313.

Kawakami S, Sato A, Nishikawa M, Yamashita F, and Hashida M (2000b) Mannose receptor-mediated gene transfer into macrophages using novel mannosylated cationic liposomes. *Gene Ther* **7**:292–299.

Kircheis R, Wightman L, Schreiber A, Robitza B, Rossler V, Kursa M, and Wagner E (2001) Polyethylenimine/DNA complexes shielded by transferrin target gene expression to tumors after systemic application. *Gene Ther* **8**:28–40.

Kichler A, Leborgne C, Coeytaux E, and Danos O (2001) Polyethylenimine-mediated gene delivery: a mechanistic study. *J Gene Med* **3**:135–144.

Klinman DM (2004) Immunotherapeutic uses of CpG oligodeoxynucleotides. *Nat Rev Immunol* **4**:1–10.

Knowles MR, Hohneker KW, Zhou Z, Olsen JC, Noah TL, Hu PC, Leigh MW, and Boucher RC (1995) A controlled study of adenoviral-vector-mediated gene transfer in the nasal epithelium of patients with cystic fibrosis. *N Engl J Med* **333**:823–831.

Krieg AM, Yi AK, Matson S, Waldschmidt TJ, Bishop GA, Teasdale R, Koretzky GA, and Klinman DM (1995) CpG motif in bacterial DNA trigger direct B-cell activation. *Nature (Lond)* **374**:546–549.

Lenardo MJ and Baltimore D (1989) NF-κB: a pleiotropic mediator of inducible and tissue-specific gene control. *Cell* **58**:227–229.

Li S, Wu SP, Whitmore M, Loeffert EJ, Wang L, Watkins SC, Pitt BR, and Huang L (1999) Effect of immune response on gene transfers to the lung via systemic administration of cationic vectors. *Am J Physiol* **276**:L796–L804.

Liu F, Qi H, Huang L, and Liu D (1997) Factors controlling the efficiency of cationic lipid-mediated transfection in vivo via intravenous administration. *Gene Ther* **6**:517–523.

Loisel S, Le Gall C, Doucet L, Ferec C, and Floch V (2001) Contribution of plasmid DNA to hepatotoxicity after systemic administration of lipoplexes. *Hum Gene Ther* **12**:685–696.

Moghimi SM, Symonds P, Murray JC, Hunter AC, Debska G, and Szewczyk A (2005) A two-stage poly(ethylenimine)-mediated cytotoxicity: implications for gene transfer/therapy. *Mol Ther* **11**:990–995.

Morimoto K, Nishikawa M, Kawakami S, Nakano T, Hattori Y, Fumoto S, Yamashita F, and Hashida M (2003) Molecular weight-dependent gene transfection activity of unmodified and galactosylated polyethylenimine on hepatoma cells and mouse liver. *Mol Ther* **7**:254–261.

Neu M, Fischer D, and Kissel T (2005) Recent advances in rational gene transfer vector design based on poly(ethylene imine) and its derivatives. *J Gene Med* **7**:992–1009.

Ross G, Erickson R, Knorr D, Motulsky AG, Parkman R, Samulski J, Straus SE, and Smith BR (1996) Gene therapy in the United States: a five-year status report. *Hum Gene Ther* **7**:1781–1790.

Sakurai F, Nishioka T, Saito H, Baba T, Okuda A, Matsumoto O, Taga T, Yamashita F, Takakura Y, and Hashida M (2001) Interaction between DNA-cationic liposome complexes and erythrocytes is an important factor in systemic gene transfer via the intravenous route in mice: the role of the neutral helper lipid. *Gene Ther* **8**:677–686.

Sakurai F, Terada T, Yasuda K, Yamashita F, Takakura Y, and Hashida M (2002) The role of tissue macrophages in the induction of proinflammatory cytokine production following intravenous injection of lipoplexes. *Gene Ther* **9**:1120–1126.

Song YK, Liu F, Chu SY, and Liu D (1997) Characterization of cationic liposome-mediated gene transfer in *vivo* by intravenous administration. *Hum Gene Ther* **8**:1585–1594.

Tan Y, Liu F, Li Z, Li S, and Huang L (2001) Sequential injection of cationic liposome and plasmid DNA effectively transfects the lung with minimal inflammatory toxicity. *Mol Ther* **3**:673–682.

Tan Y, Zhang JS, and Huang L (2002) Codelivery of NF-κB decoy-related oligodeoxynucleotide improves LPD-mediated systemic gene transfer. *Mol Ther* **6**:804–812.

Tousignant JD, Gates AL, Ingram LA, Johnson CL, Nietupski JB, Cheng SH, Eastman SJ, and Scheule RK (2000) Comprehensive analysis of the acute toxicities induced by systemic administration of cationic lipid: plasmid DNA complexes in mice. *Hum Gene Ther* **11**:2493–2513.

Tranchant I, Thompson B, Nicolazzi C, Mignet N, and Scherman D (2004) Physicochemical optimisation of plasmid delivery by cationic lipids. *J Gene Med* **6**:24–35.

Whitmore M, Li S, and Huang L (1999) LPD lipopolyplex initiates a potent cytokine response and inhibits tumor growth. *Gene Ther* **6**:1867–1875.

Wightman L, Kircheis R, Rossler V, Carotta S, Ruzicka R, Kursa M, and Wagner E (2001) Different behavior of branched and linear polyethylenimine for gene delivery in vitro and in vivo. *J Gene Med* **3**:362–372.

Yang JP and Huang L (1997) Overcoming the inhibitory effect of serum on lipofection by increasing the charge ratio of cationic liposome to DNA. *Gene Ther* **4**:950–960.

Yang Y, Nunes FA, Berencsi K, Furth EE, Gonczol E, and Wilson JM (1994) Cellular immunity to viral antigens limits E1-deleted adenoviruses for gene therapy. *Proc Natl Acad Sci USA* **91**:4407–4411.

Yew NS, Wang KX, Przybylska M, Bagley RG, Stedman M, Marshall J, Scheule RK, and Cheng SH (1999) Contribution of plasmid DNA to inflammation in the lung after administration of cationic lipid: pDNA complexes. *Hum Gene Ther* **10**:223–234.

Yew NS, Zhao H, Wu IH, Song A, Tousignant JD, Przybylska M, and Cheng SH (2000) Reduced inflammatory response to plasmid DNA vectors by elimination and inhibition of immunostimulatory CpG motifs. *Mol Ther* **1**:255–262.

Yi AK, Tuetken R, Redford T, Waldschmidt M, Kirsch J, and Krieg AM (1998) CpG motifs in bacterial DNA activate leukocytes through the pH-dependent generation of reactive oxygen species. *J Immunol* **160**:4755–4761.

Zou SM, Erbacher P, Remy JS, and Behr JP (2000) Systemic linear polyethylenimine (L-PEI)-mediated gene delivery in the mouse. *J Gene Med* **2**:128–134.

Address correspondence to: Dr. Mitsuru Hashida, Department of Drug Delivery Research, Graduate School of Pharmaceutical Sciences, Kyoto University, 46-29 Yoshidashimoadachi-cho, Sakyo-ku, Kyoto 606-8501, Japan. E-mail: hashidam@pharm.kyoto-u.ac.jp

Available online at www.sciencedirect.com
SCIENCE DIRECT®
Journal of Controlled Release 111 (2006) 333–342
journal of controlled release
www.elsevier.com/locate/jconrel

Novel PEG-matrix metalloproteinase-2 cleavable peptide-lipid containing galactosylated liposomes for hepatocellular carcinoma-selective targeting

Takeshi Terada, Mieko Iwai, Shigeru Kawakami, Fumiyoshi Yamashita, Mitsuru Hashida *

Department of Drug Delivery Research, Graduate School of Pharmaceutical Sciences, Kyoto University, Kyoto 606-8501, Japan

Received 7 May 2005; accepted 26 December 2005
Available online 20 February 2006

Abstract

In order to obtain an HCC-selective drug delivery system, a novel functional lipid, which is cleaved by the protease activity of matrix metalloproteinase-2 (MMP-2), was developed. The amino group of dioleoylphosphatidylethanolamine (DOPE) was conjugated with PEGylated MMP-2 substrate peptide (Gly–Pro–Leu–Gly–Ile–Ala–Gly–Gln), and MMP-2-cleavable PEG-Peptide-DOPE (PEG-PD) was synthesized. When PEG-PD was incorporated in galactosylated liposomes (Gal-PEG-PD-liposomes), we expected that Gal-PEG-PD-liposomes would not be taken up by normal hepatocytes due to the steric hindrance effect, but would be activated around HCC cells by secreted MMPs. In the pretreatment by hMMP2 (1, 5, and 10 μg/ml), an hMMP2 concentration-dependent higher uptake of Gal-PEG-PD-liposomes was observed in HepG2 cells, suggesting PEG-PD cleavage. In the presence of an excess of galactose, the uptake of Gal-PEG-PD-liposomes with hMMP2 was significantly inhibited, suggesting asialoglycoprotein receptor-mediated uptake of Gal-PEG-PD-liposomes following the PEG-PD cleavage. Pretreatment of Gal-PEG-PD-liposomes with the conditioned medium of B16BL6, which contained secreted MMPs, enhanced the binding to HepG2 cells, as in the case of hMMP-2 treatment. Moreover, the cytotoxicity of N^4-octadecyl-1-β-D-arabinofuranosylcytosine (NOAC) incorporated Gal-PEG-PD-liposomes was enhanced by hMMPs (5 μg/ml) and its cytotoxicity was significantly reduced by the presence of an excess of galactose in HepG2 cells. In conclusion, Gal-PEG-PD-liposomes were successfully developed for novel HCC-selective targeting.

Keywords: Matrix metalloproteinase-2; Liposomes; Targeting; PEG-Peptide-DOPE

1. Introduction

Hepatocellular carcinoma (HCC) is one of the most common malignancies worldwide and is frequently a terminal complication of chronic inflammatory and fibrotic liver disease [1]. HCC frequently shows early invasion into blood vessels as well as intrahepatic metastases, followed later by extrahepatic metastases. Intrahepatic metastasis is one of the modalities of reoccurrence within the liver in HCC. The process of invasion and metastasis of cancer cells involves several important steps: (i) detachment of the tumor cell from the primary site; (ii) invasion into blood vessels with degradation of the extracellular matrix (ECM); (iii) adhesion to blood vessels at a distant site; and (iv) invasion of the distant organs. Among them, degradation of the surrounding ECM (step (ii)) is an important step in tumor invasion and metastasis [2], and MMPs are considered to play a crucial role in this step [3,4]. In cancer research, much interest has been devoted recently to a gelatinase subgroup of MMPs that include MMP-2 (gelatinase A, M_r 72,000 type IV collagenase) and MMP-9 (gelatinase B, M_r 92,000 type IV collagenase) [5–7]. In particular, MMP-2 plays a critical role in tumor progression, angiogenesis, and metastasis [8–11]. Overexpression of MMP-2 in hepatocellular carcinoma has been shown in a number of preclinical as well as clinical investigations [12,13].

In a series of investigations, we have synthesized a novel galactosylated cholesterol derivative, cholesten-5-yloxy-*N*-(4-((1-imino-2-D-thiogalactosylethyl)amino)butyl) form-amide (Gal-C4-Chol), and demonstrated that the liposomes containing Gal-C4-Chol (Gal-liposomes) were efficiently taken up by hepatocytes via the asialoglycoprotein receptor-mediated mechanism after intravenous injection [14–16]. In the case of HCC therapy, however, although HCC cells highly express

* Corresponding author. Tel.: +81 75 753 4525; fax: +81 75 753 4575.
E-mail address: hashidam@pharm.kyoto-u.ac.jp (M. Hashida).

0168-3659/$ - see front matter © 2006 Elsevier B.V. All rights reserved.
doi:10.1016/j.jconrel.2005.12.023

asialoglycoprotein receptors, the help of Gal-liposomes is required for HCC-selective delivery; this is because galactosylated liposomes can deliver incorporated antitumor drugs not only to HCC cells but also to normal liver cells.

In the present study, therefore, we tried to develop a more HCC-selective drug delivery system in the liver. In order to achieve such a system, a novel functional lipid, which is cleaved by the protease activity of MMP-2, was exploited to activate the liposomes. The amino group of dioleoylphosphatidylethanolamine (DOPE) was conjugated with PEGylated MMP-2 substrate peptide (Gly–Pro–Leu–Gly–Ile–Ala–Gly–Gln) [17,18], and MMP-2-cleavable PEG-Peptide-DOPE (PEG-PD) was synthesized. Since the PEG chains cover the galactose ligands on the surface of the liposomes, the uptake by normal hepatocytes of Gal-liposomes containing PEG-PD (Gal-PEG-PD-liposomes) could be inhibited by steric hindrance [19]. Furthermore, the PEG chain reduces liposome uptake by macrophages of the reticuloendothelial system (RES) and extends the liposome half-time of the circulation [20]. In the HCC cells, on the other hand, the PEG-PD in Gal-PEG-PD-liposomes can be cleaved by MMP-2, exposing the galactose moieties on the liposomal surface; consequently, they can be selectively recognized by asialoglycoprotein receptors on HCC cells.

We describe here the uptake characteristics of Gal-PEG-PD-liposomes by cultured HepG2 cells after pretreatment with purified human MMP-2 (hMMP-2) and conditioned medium of mouse melanoma cells (B16BL6), known to highly express MMPs [21]. Furthermore, N^4-octadecyl-1-β-D-arabinofuranosylcytosine (NOAC), which is a lipophilic derivative of ara-C [22–24], was incorporated in Gal-PEG-PD-liposomes, and its cytotoxicity against cultured HepG2 cells was evaluated.

2. Materials and methods

2.1. Materials

N-(4-aminobutyl) carbamic acid *tert*-butyl ester was purchased from Tokyo Chemical Industry (Tokyo, Japan). Distearoyl phosphatidylcholine (DSPC), DOPE, cholesteryl chloroformate, 3-(4,5-dimethylthiazol-2-yl)-2,5-diphenyltetrazolium bromide (MTT), ara-C, and NOAC were purchased from Sigma-Aldrich Co. (St. Louis, MO, USA). Chol and Clear-Sol I was obtained from Nacalai Tesque Inc. (Kyoto, Japan), and Soluene 350 was purchased from Packard Bioscience Co. (Groningen, Netherlands). [^{3}H] CHE was purchased from NEN Life Science Products Inc. (Boston, MA, USA). L-α-Phosphatidylethanolamine-*N*-fluorescein (PE-fluorescein) was purchased from Avanti Polar Lipids Inc. (Alabama, AL, USA). Two-imino-2-methoxyethyl-L-thiogalactoside was synthesized as reported previously [25]. MMP-2-cleavable peptide (Gly–Pro–Leu–Gly–Ile–Ala–Gly–Gln) was custom-made by Toray Research Center Inc. (Tokyo, Japan). Methoxy-poly (ethylene glycol)-*N*-hydroxysuccinimide (mPEG-NHS) was purchased from NOF Co. Inc. (Tokyo, Japan). All other chemicals were reagent grade products obtained commercially.

2.2. Synthesis of PEG-PD

PEG-PD was synthesized by reacting the peptide (Gly–Pro–Leu–Gly–Ile–Ala–Gly–Gln) containing MMP-2-cleavable sequences with each chain length of mPEG-NHS and then with DOPE. Briefly, the peptide and each chain length of mPEG-NHS with each molecular weight (1.2 : 1, molar ratio) were mixed and stirred in carbonate buffer (pH 8.5) at 4 °C overnight. After dialysis and lyophilization, the reacted powder (mPEG-peptide) and DOPE (1 : 1, molar ratio) in chloroform: tetrahydrofuran (1 : 4, v/v) were reacted overnight by adding 1.2-equal mol of 1,3-dicyclohexyl-carbodiimide (DCC) and 1-hydroxybenzotriazole (HOBt) at room temperature. TLC analysis and ninhydrin assay showed that the reaction had gone to completion. After filtration of the precipitate, a powder of PEG-PD was obtained after evaporation of the solvent. After dialysis in distilled water and lyophilization, the material was used in the next step.

MMP-2-uncleavable PEG-DOPE (PEG-D) was synthesized by reacting mPEG-NHS with DOPE. The purity of each synthesized PEG-lipid was calculated by phosphate assay and was >80% on the basis of DOPE.

2.3. Synthesis of Gal-C4-Chol

Gal-C4-Chol was synthesized according to the method reported previously [26]. Cholesteryl chloroformate and *N*-(4-aminobutyl)carbamic acid *tert*-butyl ester were reacted in chloroform for 24 h at room temperature. After the reaction mixture was incubated with trifluoroacetic acid for 4 h at 4 °C, the solvent was evaporated to give *N*-(4-aminobutyl)-(cholesten-5-yloxyl)formamide, which was reacted with an excess of 2-imino-2-methoxyethyl-1-thiogalactoside [25] in pyridine containing triethylamine for 24 h at room temperature. After the reaction mixture was evaporated, the resultant material was suspended in water and dialyzed against distilled water for 48 h using a dialysis membrane (12-kDa cutoff).

2.4. Preparation of liposomes

Each lipid mixture (DSPC, Chol, Gal-C4-Chol, and PEG-PD) was dissolved in chloroform and evaporated to dryness. [^{3}H] CHE or PE-fluorescein (1 mol %) was added to the liposomes for the uptake study and confocal microscopy, respectively. The dried lipid films were hydrated in HBS (50 mM HEPES, 150 mM NaCl, pH 7.4) containing 5 mM $CaCl_2$ and sonicated at 65 °C for 3 min. The lipid concentration was monitored by phosphate assay. The mean vesicle diameters of the liposomes were determined using a laser light scattering size analyzer (LS-900, Otsuka Electronics Co. Ltd., Osaka, Japan).

2.5. Gelatin zymography assay

B16BL6 cells (1×10^6) were seeded onto 100 mm tissue culture dishes and allowed to adhere in the presence of serum. Subsequently, medium was replaced by 10 mL serum-free

DMEM per well. After 72h of incubation, the conditioned medium was collected and ultracentrifuged to remove the cell debris. The supernatants concentrated by 10-kDA cutoff VIVA SPIN (Vivascience, Hannover, Germany) were used for MMP-2 detection by zymography [27]. Purified hMMP-2 (Chemicon, California, USA) was used as a migration standard for the assays.

2.6. PEG-PD cleavage assay in PEG-PD-liposomes

PEG-PD cleavage by MMP-2 was checked by evaluating the amino residues appearing following digestion of PEG-PD. TLC detection and the TNBS method were used for PEG-PD cleavage assay of hMMP-2 and the conditioned medium of B16BL6 cells, respectively. In the hMMP-2 digestion, 4mM liposome samples were incubated with 5μg/ml active hMMP-2 (activated with *p*-aminophenylmercuric acetate for 1h) in 1ml HBS containing 5mM $CaCl_2$ at 37°C for 24h. After ultracentrifugation at 50000 ×*g* for 10min at 4 °C in a Himac CS100EX ultracentrifuge (Hitachi, Ltd., Tokyo, Japan) and washing 3 times with saline, the lipid pellets were resuspended in chloroform and spotted onto TLC plates. TLC was carried out with a chloroform:methanol (75:25) mobile phase, followed by air drying, and visualization by ninhydrin. In the conditioned medium, B16BL6 cells were cultured with serum-free DMEM for 72h. Subsequently, the supernatants were collected and ultracentrifuged to remove the cell debris. The supernatants concentrated by 10-kDa cutoff VIVA SPIN were used for MMP-2 detection by zymography and PEG-PD cleavage assay. Four mM samples of liposomal suspensions were diluted twice with the conditioned medium of B16BL6 cells in the absence or presence of 25nM GM6001 (Chemicon, California, USA) then incubated at 37°C. At each time point, the liposomal suspensions were centrifuged and washed as described for the TLC detection; also, 4mM samples of the liposomal suspensions were analyzed by the TNBS method [28].

2.7. Cellar uptake of Gal-PEG-PD-liposomes in HepG2 cells

HepG2 cells were plated on 12-well culture plates at a density of 5×10^5 cells/well. After 24h cultivation, cells were washed three times and preincubated for 20min with Hanks' balanced salt solution (HBSS). Then, 4mM samples of liposomes were incubated with various concentrations of hMMP-2 or conditioned medium of B16BL6 cells for 24h as described above. After pre-incubation, the cells were incubated at 37°C for 2h with HBSS containing treated [^{3}H] liposomes (100μM, 3.0MBq/ml). For the inhibition study, 20mM galactose was added to both solutions for the preincubation and liposome suspensions. At the end of the incubation period, the medium was removed and the cells were washed 5 times with cold HBSS. The cells were then solubilized with 0.5ml 1 N NaOH solution overnight and then neutralized with 0.1ml 5 N HCl solution. The radioactivity of the [^{3}H] CHE was measured in a scintillation counter (LSA-500, Beckman, Tokyo, Japan). The protein content was also measured using a Protein Quantification Kit (Dojindo Molecular Technologies, Inc., Gaithersburg, MD, USA). In the case of the confocal microscopy study, the cells were incubated at 37°C for 1h with fluorescein-labeled liposomes and examined by confocal laser microscopy (MRC-1024; Bio-Rad, California, USA).

2.8. Cellar uptake of Gal-PEG-PD-liposomes in primary cultured macrophages

Each sample of liposomes was prepared in HBSS as described above. The prepared liposomes were extruded 5 times through 200 and 100nm pore-size polycarbonate membranes at 65°C. The mean vesicle diameters were confirmed to be about 100nm using a laser light scattering size analyzer. Five-week-old male ICR mice were obtained from Shizuoka Agricultural Co-operative Association for Laboratory Animals (Shizuoka, Japan). All animal procedures were examined by the Ethics Committee on Animal Experiment at the Kyoto University. Resident macrophages were collected from the peritoneal cavity of unstimulated mice with serum-free RPMI 1640 medium [29]. Washed cells were suspended in RPMI 1640 medium supplemented with serum and plated on 12-well culture plates at a density of 1×10^6 cells/well. After incubation for 2h at 37 °C in 5% CO_2–95% air, adherent macrophages were washed three times with RPMI 1640 medium to remove nonadherent cells and then cultured under the same conditions. After 48h cultivation, the cells were washed 3-times and incubated with HBSS containing treated [^{3}H] liposomes (200μM, 3.0MBq/ml) at 37°C for 2h. The radioactivity was measured as described above.

2.9. Stability of Gal-PEG-PD-liposomes in fetal bovine serum (FBS)

Liposome samples were prepared in HBSS and extruded as described above. Four mM liposome samples were diluted twice with fetal bovine serum (Flow Laboratories, Irvine, UK) and incubated at 37°C. At each time point, the change in particle diameter was measured using a laser light scattering size analyzer.

2.10. Cytotoxicity assay of NOAC incorporated Gal-PEG-PD-liposomes in HepG2 cells

Four mM DSPC/Chol/Gal/PEG-PD/NOAC (60:24.5:5:0.5:10) liposome samples were incubated with 5μg/ml hMMP-2 as described above. HepG2 cells were counted and seeded in 96-well plates (5×10^4 cells/well). After 24h incubation, cells were exposed to serum-free DMEM containing various concentration (0–400μM) of ara-C, NOAC or empty PEG-PD-liposomes in the case of pretreatment or no treatment with hMMP-2 for 24h at 37 °C. The cytotoxic effects were determined by MTT dye reduction assay as described by Mosmann [30]. In the inhibition study, the cells were exposed to each of the conditioned liposome samples in the presence or absence of 20mM galactose for 2h at 37°C and then the medium was changed to DMEM supplemented with serum. After 24h incubation, the cytotoxic effects were determined by MTT dye reduction assay (Table 1).

Table 1
Lipid composition and mean particle size of the tested liposomes

Lipid composition (molar ratio)	Particle size (nm)[a]
Gal-liposomes (DSPC/Chol/Gal-C4-Chol=60:35:5)	120.9±4.9
Gal-PEG-PD-liposomes (DSPC/Chol/Gal-C4-Chol/PPD=60:34.99:5:0.01)	110.4±6.6
Gal-PEG-PD-liposomes (DSPC/Chol/Gal-C4-Chol/PPD=60:34.9:5:0.1)	105.1±0.91
Gal-PEG-PD-liposomes (DSPC/Chol/Gal-C4-Chol/PPD=60:34.5:5:0.5)	107.1±3.2
Gal-PEG-PD-liposomes (DSPC/Chol/Gal-C4-Chol/PPD=60:34:5:1)	106.3±9.5

[a] The mean particle sizes of the liposomes were measured using a laser light scattering particle size analyzer. Results are expressed as the mean±S.D. of three experiments.

2.11. Statistical analysis

Statistical comparisons were performed by Student's *t*-test for two groups, and one-way ANOVA for multiple groups. $P<0.05$ was considered to be indicative of statistical significance.

3. Results

3.1. Cleavage of PEG-PD-liposomes by preincubation with hMMP-2 or conditioned medium of B16BL6

Cleavage by hMMP-2 to release the PEG coating of PEG-PD-liposomes was tested by TLC assay. The spot of the PEG-PD-liposomes incubated with hMMP-2 on the TLC plate was visualized by ninhydrin reagent, suggesting that NH_2-IAGQ-DOPE is produced by the cleavage (data not shown).

The preincubation of PEG-PD-liposomes with the conditioned medium of B16BL6, known to be cells that highly secrete MMPs, resulted in the cleavage of PEG-PD. Gelatin zymography was employed to confirm that the conditioned medium contained MMP-2 (Fig. 1A). The result of the TNBS assay demonstrated a time-dependent cleavage of PEG-PD and appearance of NH_2-IAGQ-DOPE (Fig. 1B). In contrast, MMP-2-uncleavable PEG-DOPE (PEG-D), which is synthesized by reacting mPEG-NHS with DOPE, was negative. In addition, inhibition of the cleavage by GM6001, known to inhibit MMPs, and the negative results of PD-liposomes suggested that the cleavage was specifically by MMPs present in conditioned medium of B16BL6 (Fig. 1C).

3.2. Activated binding of Gal-PEG-PD-liposomes with HepG2 cells by hMMP-2 or conditioned medium of B16BL6 cells

Gal-liposomes showed a high uptake via the asialoglycoprotein receptor-mediated process by HepG2 cells, but hMMP-2 treatment had no effect on this uptake (Fig. 2A). On the other hand, Gal-PEG-PD (0.1%)-liposomes after pretreatment with hMMP-2 exhibited a higher uptake by HepG2 cells, compared with the non-treatment group. In addition, inhibition of the higher uptake by 20 mM galactose suggested that the increase in the uptake was due to asialoglycoprotein receptor-mediated uptake by galactose ligands on the surface of the liposomes. Pretreatment of Gal-PEG-PD-liposomes with conditioned medium of B16BL6 enhanced the binding to HepG2 cells, as in the case of hMMP-2 treatment (Fig. 2B). In addition, the

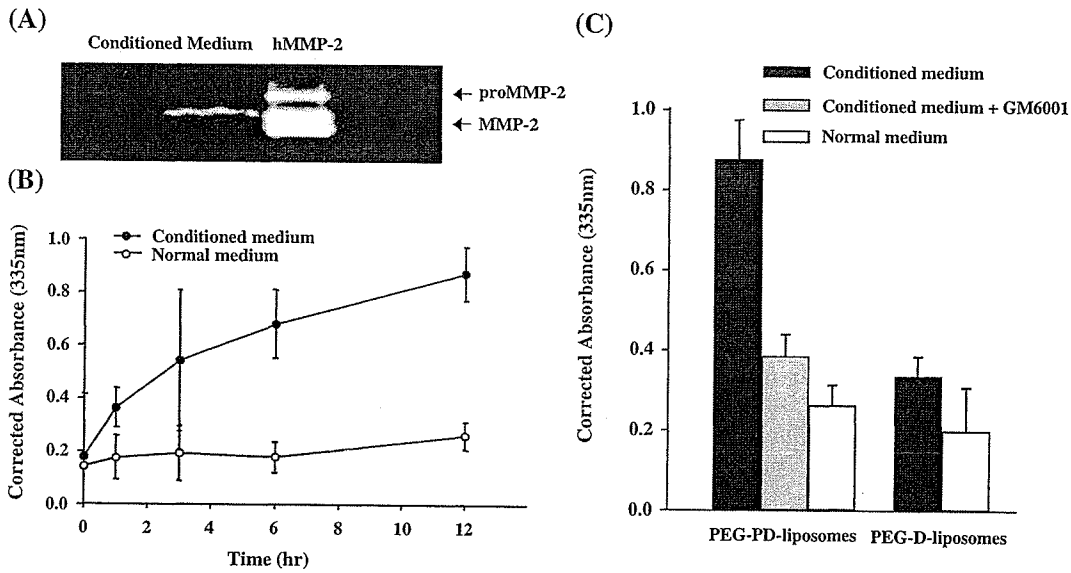

Fig. 1. Quantitation of the cleavage of PEG-PD by the conditioned medium of B16BL6 cells. (A), Zymography of secreted MMP-2 in the conditioned medium of B16BL6 cells. The right and left lanes show hMMP-2 as the standard and the conditioned medium, respectively. The amino residues appearing through digestion of PEG-PD were determined by the TNBS method. (B), Cleavage kinetics of DSPC/Chol/PEG-PD (60:35:5) liposomes incubated with the conditioned (●) and normal (○) medium. (C), Each liposome sample was incubated with the conditioned (filled) and normal (open) medium for 12 h at 37 °C. In the case of Gal-PEG-PD-liposomes, GM6001 was added to the conditioned medium as an MMP inhibitor (hatched). Each result represents the mean±S.D. of three experiments.

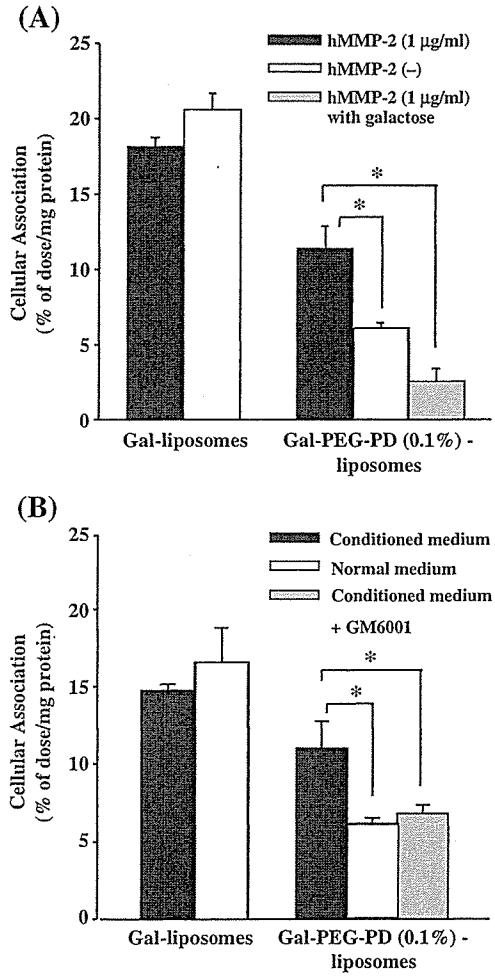

Fig. 2. Effect of MMP pretreatment on the uptake of liposomes (100 μM) by HepG2 cells. (A), [^{3}H] liposomes were incubated with (filled) or without (open) 1 μg/ml hMMP-2 used in the uptake study. Then, galactose was used to inhibit the uptake (hatched). (B), [^{3}H] liposomes incubated with the conditioned medium of B16BL6 cells (filled) or normal medium (open) used in the uptake study. GM6001 was added to the conditioned medium as an inhibitor of MMPs (hatched). Each result represents the mean±S.D. of three experiments. *Statistically significant differences ($P<0.05$).

higher uptake of PEG-PD-liposomes after treatment with conditioned medium was inhibited in the presence of GM6001. This suggests that MMPs secreted by B16BL6 cells can cleave PEG-PD, and then the liposomes will be taken up via galactose ligands on the surface by HepG2 cells.

3.3. The effect of PEG-PD content and its hMMP stability on the binding of Gal-PEG-PD-liposomes in HepG2 cells

Since the steric hindrance effect by PEG-PD is expected to depend on the amount of PEG-PD in Gal-PEG-PD-liposomes, the uptake of Gal-PEG-PD-liposomes with various amounts of PEG-PD was examined in HepG2 cells (Fig. 3). In Gal-PEG-PD-liposomes with 0.5% and 1% PEG-PD, the binding to HepG2 was significantly inhibited, suggesting a steric hindrance effect. Therefore, at least 0.5% PEG-PD is required to avoid recognition by asialoglycoprotein receptors on normal hepatocytes.

In the HCC-selective targeting system, the uptake by normal hepatocytes of Gal-PEG-PD-liposomes needs to be reduced, that is, the steric hindrance effect by PEG-PD in the blood circulation is very important. A previous study has reported that the serum MMP-2 concentrations in HCC patients are higher than those in healthy subjects, and the value has been reported to be about 1 μg/ml [13]. Therefore, we evaluated the effect of 1 μg/ml MMP-2 on the uptake by HepG2 cells. In the presence of 1 μg/ml hMMP-2, the cellular uptake of Gal-PEG-PD-liposomes with 0.01% and 0.1% PEG-PD was significantly higher than that in the absence of hMMP-2, suggesting the degradation of PEG-PD in Gal-PEG-PD-liposomes. However, the cellular uptake of Gal-PEG-PD-liposomes with 0.5% and 1% PEG-PD was not enhanced by treatment with 1 μg/ml hMMP-2, suggesting that Gal-PEG-PD (0.5 and 1%)-liposomes are stable in blood. Such steric characteristics of Gal-PEG-PD (0.5 and 1%)-liposomes can enhance the HCC-selectivity. Thus, Gal-PEG-PD (0.5%)-liposomes were selected for the following experiments.

3.4. The effect of hMMP-2 concentration on the binding of Gal-PEG-PD-liposomes in HepG2 cells

In our HCC-selective targeting system, PEG-PD in Gal-PEG-PD (0.5%)-liposomes needs to be degraded by a higher concentration of hMMP-2, i.e. >1 μg/ml (serum MMP-2 concentration of HCC patients). Thus, the effect of hMMP-2 concentration on the binding of Gal-PEG-PD-liposomes to HepG2 cells was evaluated. The binding of Gal-PEG-PD-liposomes to HepG2 cells was significantly enhanced in an hMMP-2 concentration-dependent manner (Fig. 4). Especially, the treatment with 5 and 10 μg/ml hMMP-2 significantly enhanced the uptake of Gal-PEG-PD (0.5%)-liposomes by HepG2 cells. The confocal microscopy study also showed that

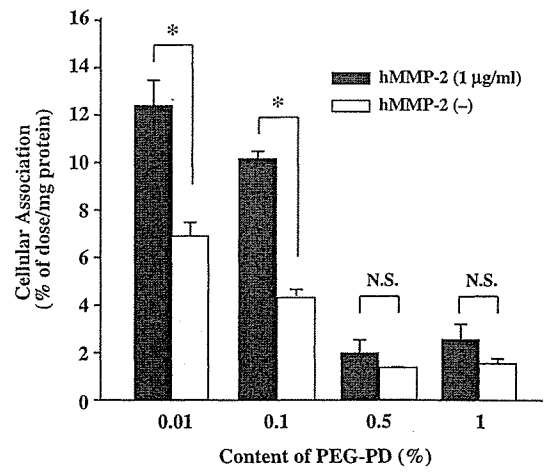

Fig. 3. Effect of PEG-PD content and hMMP-2 stability on the uptake of Gal-PEG-PD-liposomes by HepG2 cells. [^{3}H] Gal-PEG-PD-liposomes were incubated with 1 μg/ml hMMP-2. Each result represents the mean±S.D. of three experiments.

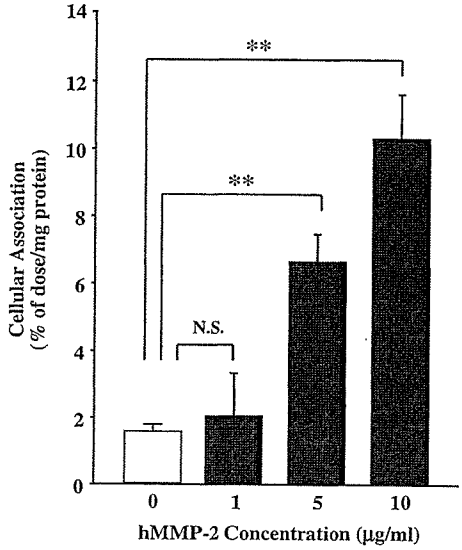

Fig. 4. Effect of hMMP-2 concentration on the uptake of Gal-PEG-PD-liposomes by HepG2 cells. [^{3}H] Gal-PEG-PD-liposomes were incubated with 1, 5, and 10 μg/ml hMMP-2. Each result represents the mean±S.D. of three experiments.

the uptake of Gal-PEG-PD (0.5%)-liposomes by HepG2 was enhanced by the treatment of 5 μg/ml hMMP-2 (Fig. 5A) and completely inhibited in the case of no treatment (Fig. 5B). These results suggest that the cleavage by 5 μg/ml hMMP-2 is required to achieve the significant uptake of Gal-PEG-PD (0.5%)-liposome by HepG2 cells.

3.5. The effect of PEG-PD on the binding of Gal-PEG-PD-liposomes in primary cultured macrophages and the stability of liposomal size in FBS

To evaluate the non-specific uptake of Gal-PEG-PD-liposomes by RES, mouse peritoneal macrophages were used as a model of mononuclear phagocytes in the RES. The uptake of Gal-liposomes by peritoneal macrophages was significantly inhibited by the incorporation of PEG-PD, and the effect was dependent on the amount of PEG-PD (Fig. 6A), suggesting the reduced non-specific uptake of Gal-PEG-PD-liposomes by RES.

Moreover, PEG-PD enhanced the stability of liposomes in the serum (Fig. 6B). The particle size of Gal-liposomes quickly increased after incubation with FBS. On the other hand, the size of Gal-PEG-PD-liposomes could sustain a particle size of 100 nm. In particular, the size of Gal-PEG-PD-liposomes with 0.5% PEG-PD was constant even 24 h after incubation, suggesting that Gal-PEG-PD (0.5%)-liposomes are stable in the body.

3.6. The cytotoxicity of NOAC incorporated in Gal-PEG-PD-liposomes in HepG2 cells

In order to evaluate the cytotoxicity of Gal-PEG-PD (0.5%)-liposomes in HepG2 cells, NOAC, a lipophilic derivative of ara-C, was incorporated into Gal-PEG-PD-liposomes (Fig. 7). The cytotoxicity of NOAC incorporated into Gal-PEG-PD (0.5%)-liposomes with the hMMP-2 (5 μg/ml) was significantly more cytotoxic than that without hMMP-2, suggesting that the higher cytotoxicity resulted from the degradation of PEG-PD. In the presence of 20 mM galactose, the cytotoxicity of NOAC incorporated into Gal-PEG-PD-liposomes with hMMP-2 treatment was significantly inhibited, suggesting that asialoglycoprotein receptor-mediated uptake is involved in the cytotoxicity of NOAC incorporated into Gal-PEG-PD (0.5%)-liposomes.

Fig. 8 shows the concentration-dependent cytotoxicity of NOAC, Gal-PEG-PD (0.5%)-liposomes, NOAC incorporated into Gal-PEG-PD (0.5%)-liposomes with or without hMMP-2 in HepG2 cells. In these NOAC concentration ranges, the cytotoxicity of NOAC incorporated into Gal-PEG-PD (0.5%)-liposomes was higher than that of NOAC and/or Gal-PEG-PD (0.5%)-liposomes. Furthermore, hMMP-2 treatment enhanced the cytotoxic effect of NOAC incorporated into Gal-PEG-PD (0.5%)-liposomes, suggesting that the

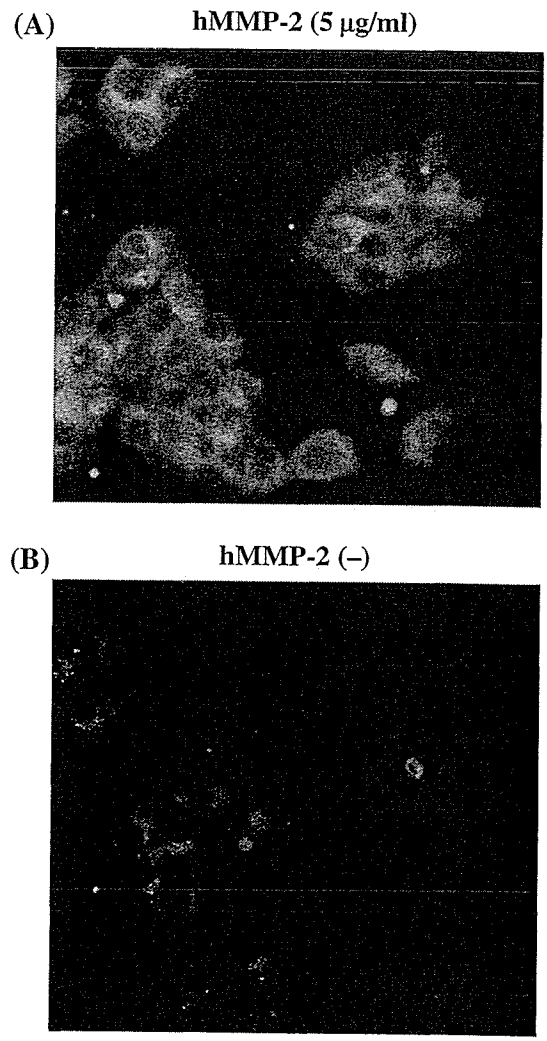

Fig. 5. Confocal microscopic image of Gal-PEG-PD-liposomes with (A) or without (B) hMMP-2 (5 μg/ml) in HepG2 cells. Conditioned Gal-PEG-PD-liposomes containing 1% PE-fluorescein were incubated with HepG2 cells for 1 h. (A), treatment with 5 μg/ml hMMP-2. (B), no treatment.

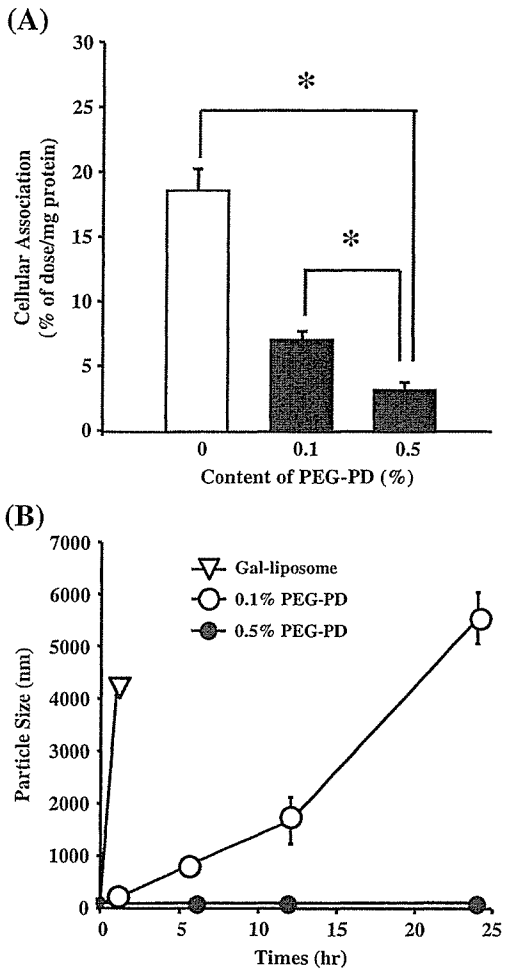

Fig. 6. Effect of PEG-PD content in Gal-liposomes on the uptake by peritoneal macrophages and the stability in FBS. (A), The uptake study of [^{3}H] Gal-PEG-PD-liposomes with 0.1, and 0.5% PEG-PD or without PEG-PD (Gal-liposomes) in peritoneal macrophages was carried out. Each result represents the mean±S.D. of three experiments or three wells. *Statistically significant differences ($P<0.05$). (B), The particle size of each Gal-PEG-PD-liposomes with 0.1 (○), and 0.5 (●) % PEG-PD or without PEG-PD (▽) was measured at each time point after incubation with an equal volume of FBS.

higher cytotoxicity resulted from the cleavage of PEG-PD. Thus, these results suggest that NOAC incorporated into Gal-PEG-PD (0.5%)-liposomes with hMMP-2 is taken up by asialoglycoprotein receptor-mediated endocytosis following the cleavage of PEG-PD.

4. Discussion

We have described a novel PEGylated liposome approach, in which the protease activity of MMP-2 is exploited to release PEG coating and expose the tumor targeting ligand on the surface, as a drug delivery system for tumor therapy. Until now, an MMP cleavable linker has often been used as an effective targetable strategy to trigger the targeting of antitumor drugs or retroviral vectors to tumor tissues [31–34]. Recently, some groups have applied the MMP cleavable linker to dextran and hydrogel as MMPs triggered drug delivery carrier [35,36]. On

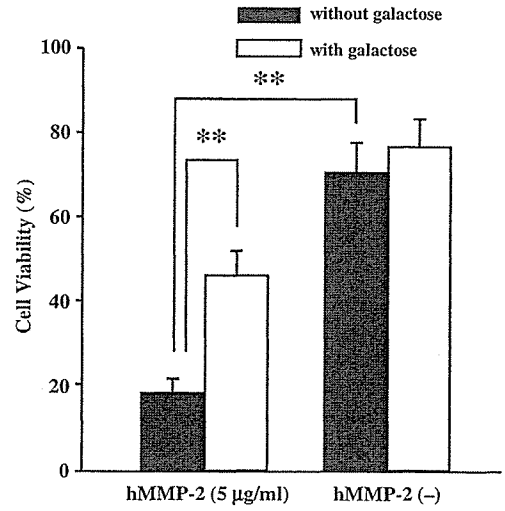

Fig. 7. Cytotoxicity of NOAC incorporated Gal-PEG-PD-liposomes by activation of hMMP-2 (5 μg/ml) in HepG2 cells. HepG2 cells were incubated with hMMP-2 treated liposomes, no treated liposomes in the absence (■) or presence (□) of galactose. Cytotoxicity was evaluated by MTT assay. Each result represents the mean±S.D. of three wells. **Statistically significant differences ($P<0.01$).

the other hand, liposomes are the most extensively studied of all particulate carriers, and several commercial products are now available. This is because liposomes are easily prepared and have a large capacity even for hydrophobic drugs. Our present report is the first study of MMP activated delivery via liposomes.

MMP-2 mediated cleavage of PEG-PD contained in liposomes is the essential step to success in our strategy. Therefore, the step was confirmed by using TLC assay and the TNBS method (Fig. 1). MMP-2 treatment hydrolyzed the peptide between DOPE and PEG and resulted in the conversion of PEG-PD to NH_2-Ile-Ala-Gly-Gln-DOPE. The core of the

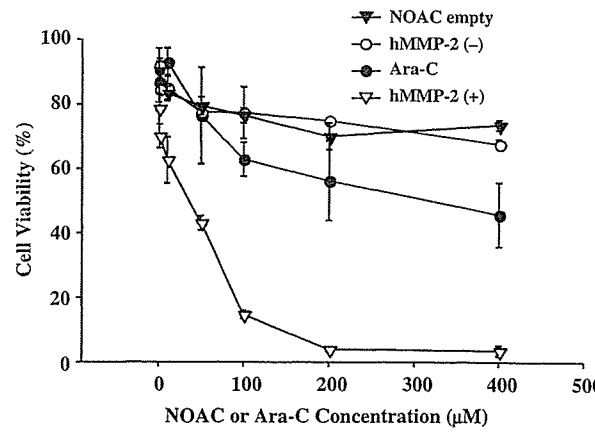

Fig. 8. Effect of NOAC concentration on the cytotoxicity of NOAC incorporated Gal-PEG-PD-liposomes in HepG2 cells. HepG2 cells were incubated with hMMP-2 treated NOAC incorporated Gal-PEG-PD-liposomes (▽), no treated NOAC incorporated Gal-PEG-PD-liposomes (○), Ara-C (●) and empty Gal-PEG-PD-liposomes (▼) at a concentration ranging from 0.1 to 400 μM NOAC. After incubation, cytotoxicity was evaluated by MTT assay. Each result represents the mean±S.D. of three experiments.

cleavage site (PLGI) is also cleaved by MMP-3, MMP-7, MMP-8, and MMP-9 [37]. The cleavage of PEG-PD by MMPs secreted by tumor cells was also confirmed. The conditioned medium of B16BL6 cells, generally known as cells over-expressing MMPs, was used for this study. It was confirmed that the conditioned medium contained MMP-2 by using gelatin zymography (Fig. 1A). The cleavage of PEG-PD was promoted time-dependently following treatment of the B16BL6 conditioned medium (Fig. 1B). The cleavage seemed to occur at the MMP-2-cleavable peptide contained in PEG-PD, since PEG-D without the peptide underwent no cleavage following treatment with the conditioned medium. Moreover, since co-incubation with enough GM6001, a known MMP inhibitor [38], led to a reduction in the cleavage, this suggests that the cleavage is due to MMPs contained in the conditioned medium (Fig. 1C).

Gal-PEG-PD-liposomes subjected to the cleavage step of PEG-PD by MMP-2 need specific uptake via the asialoglycoprotein receptors on HCC cells. The higher uptake of PEG-PD (0.1%)-Gal-liposomes incubated with hMMP-2 compared with that of the no hMMP-2 treatment group by HepG2 cells, was inhibited in the presence of 20 mM galactose, suggesting that the increase in the uptake is due to an asialoglycoprotein receptor-mediated uptake mechanism via the galactose ligands exposed on the surface of the liposomes after the cleavage of PEG-PD by hMMP-2 (Fig. 2A). The increasing uptake was not due to bridging between the liposomes and cells by hMMP-2, because the degree of uptake of Gal-liposomes without PEG-PD, incubated and not incubated with hMMP-2, was almost identical. A similar effect was confirmed using conditioned medium (Fig. 2B). The added GM6001 reduced the uptake of Gal-PEG-PD-liposomes by HepG2 cells, as the reagent was able to inhibit the cleavage of PEG-PD by MMPs.

Though the serum MMP-2 concentration of HCC patients has been reported to be about 1 μg/ml [13], it is difficult to accurately determine the local concentration of MMP-2 in tumor tissues. However, some groups have demonstrated the strong expression of MMP-2 in HCC tumor tissues [13,39], and it has reported that active form of MMP-2 is more strongly expressed by HCC than by noncancerous tissues. In addition, Murawaki et al. have reported that the elevation of serum MMP-2 concentration in the HCC patients is considered to be derived from the underlying liver cirrhosis [13]. Therefore, we considered that the intratumoral concentration of MMPs might be some times higher than the serum concentration (1 μg/ml), and the studies using the higher concentrations (5 and 10 μg/ml) were also conducted. Gal-PEG-PD (0.01 or 0.1%)-liposomes treated for 24 h by 1 μg/ml hMMP-2 exhibited a higher uptake, compared with no treatment groups (Fig. 3). On the other hand, Gal-PEG-PD (0.5%)-liposomes completely masked the galactose ligands on the surface and inhibited the uptake by HepG2 cells, and treatment for 24 h with 1 μg/ml hMMP-2 was not enough to release a significant amount of PEG-PD and lead to the subsequent uptake via exposed galactose ligands on the surface by HepG2 cells. However, treatment for 24 h with high concentrations of hMMP-2 (5 and 10 μg/ml) led to a significantly high uptake (Figs. 4 and 5). Our results led us to surmise that, in the therapy of HCC patients, Gal-PEG-PD (0.5%)-liposomes can completely mask the galactose ligands on the surface under the circulation in the body other than MMP-2 concentrated tumor tissues, that is the condition of low MMP-2 concentration, suggesting that the non-expectant uptake by normal liver PC would be maximally reduced. The lipophilic derivatives of antitumor drugs are stably retained in liposomes. In particular, NOAC is a new lipophilic derivative able to overcome the disadvantage of rapid degradation of ara-C to the biologically inactive metabolite 1-β-D-arabinofuranosyluracil (ara-U) and it has potent antitumor activity against solid tumors [21–23]. In our studies, although Gal-PEG-PD-liposomes containing 10% NOAC had no cytotoxic effect on HepG2 cells, the hMMP-2 pretreatment group exhibited a significant cytotoxic effect (Fig. 7). These results suggest that MMP-2 can release the PEG coating preventing the uptake of NOAC, and the subsequently exposed galactose ligand on the surface can induce the uptake in the same way as in the binding study of Gal-PEG-PD-liposomes and enhance the antitumor effect. The inhibition study in presence of galactose supports this theory. A dose-dependent cytotoxic effect was found in the hMMP-2 pretreatment group, but not in the no treatment group and for Gal-PEG-PD-liposomes without NOAC (Fig. 8). The higher cytotoxic effect of the hMMP-2 pretreatment group compared with that of ara-C in this in vitro study confirmed the report that N^4-alkyl-ara-C derivatives are active at lower concentrations compared with ara-C [40].

The PEGylation of liposomes leads to a reduction in the non-specific uptake by RES and subsequent prolongation of the circulation lifetime. In practical terms, our study demonstrated that 0.5% of PEG-PD, which undergoes cleavage by MMP-2, significantly reduced the uptake of Gal-liposomes by peritoneal macrophages, compared with 0% or 0.1% PEG-PD (Fig. 6A). In addition, Gal-PEG-PD (0.5%)-liposomes exhibited a higher retention of the particle size in the presence of serum (Fig. 6B). The smaller particle size (~200 nm) of liposomes reduces the unspecific uptake by RES. These results would lead to prolonged circulation and tumor-selective enhanced permeability and retention of Gal-PEG-PD (0.5%)-liposomes. Some recent studies have reported that, although PEG can act directly as a steric barrier in the interaction of the liposomes with macrophages and offer a prolonged lifetime, the reduction effect against adsorption of plasma proteins could not be obtained by modification [41,42]. Those studies support our strategy that secreted MMP-2 around HCC tissues can recognize the cleavable side of the novel PEGylated liposomes obtaining prolonged circulation and release the PEG coating.

The successful transfer of Gal-PEG-PD-liposomes into HepG2 cells by MMP-2 treatment is likely to be very useful for the delivery of antitumor drugs to HCC tissues. On the other hand, it has been reported the overexpression of MMP-9 in addition to MMP-2 in HCC tissues [43]. Since the conjugated peptide could be also cleaved by MMP-9 [18], Gal-PEG-PD-liposome is capable of HCC-selective drug delivery via the PEG-PD cleavage not only by MMP-2, but also by MMP-9. Recently, some novel MMP-2 substrates have been investigated using peptide libraries and peptide phage libraries [32,44]. In our strategy, the more specific substrates for MMP-2 are capable

of enhancing the efficiency of drug delivery to tumor tissues. Moreover, many reports have described the successful development of drug delivery systems using specific ligands for the receptors overexpressed by some tumor types, such as folate and transferrin [45,46]. These may represent further applications for our strategy.

Acknowledgments

This work was supported in part by Grants-in-Aid for Scientific Research from Ministry of Education, Culture, Sports, Science, and Technology of Japan, and by Health and Labor Sciences Research Grants for Research on Hepatitis and BSE from the Ministry of Health, Labor and Welfare of Japan, and by Technology of Japan and by 21st Century COE Program "Knowledge Information Infrastructure for Genome Science".

References

[1] D.F. Schafer, M.F. Sorrell, Hepatocellular carcinoma, Lancet 353 (1999) 1253–1257.
[2] N. Theret, O. Musso, B. Turlin, D. Lotrian, P. Bioulac-Sage, J.P. Campion, K. Boudjema, B. Clement, Increased extracellular matrix remodeling is associated with tumor progression in human hepatocellular carcinomas, Hepatology 34 (2001) 82–88.
[3] C. Yang, M. Zeisberg, J.C. Lively, P. Nyberg, N. Afdhal, R. Kalluri, Integrin α1β1 and α2β1 are the key regulators of hepatocarcinoma cell invasion across the fibrotic matrix microenvironment, Cancer Res. 63 (2003) 8312–8317.
[4] H. Sato, T. Takino, Y. Okada, J. Cao, A. Shinagawa, E. Yamamoto, M. Seiki, A matrix metalloproteinase expressed on the surface of invasive tumour cells, Nature 370 (1994) 61–65.
[5] T. Takahara, K. Furui, Y. Yata, B. Jin, L.P. Zhang, S. Nambu, H. Sato, M. Seiki, A. Watanabe, Dual expression of matrix metalloproteinase-2 and membrane-type 1-matrix metalloproteinase in fibrotic human livers, Hepatology 26 (1997) 1521–1529.
[6] A. Hayasaka, N. Suzuki, N. Fujimoto, S. Iwama, E. Fukuyama, Y. Kanda, H. Saisho, Elevated plasma levels of matrix metalloproteinase-9 (92-kd type IV collagenase/gelatinase B) in hepatocellular carcinoma, Hepatology 24 (1996) 1058–1062.
[7] Y. Murawaki, Y. Ikuta, K. Okamoto, K. Mimura, M. Koda, H. Kawasaki, Plasma matrix metalloproteinase-9 (gelatinase B) in patients with hepatocellular carcinoma, Res. Commun. Mol. Pathol. Pharmacol. 108 (2000) 35–17.
[8] A.F. Chambers, L.M. Matrisian, Changing views of the role of matrix metalloproteinases in metastasis, J. Natl. Cancer Inst. 89 (1997) 1260–1270.
[9] S. Curran, G.I. Murray, Matrix metalloproteinases in tumour invasion and metastasis, J. Pathol. 189 (1999) 300–308.
[10] U.B. Hofmann, J.R. Westphal, G.N.P. van Muijen, D.J. Ruiter, Matrix metalloproteinases in human melanoma, J. Investig. Dermatol. 115 (2000) 337–344.
[11] U.B. Hofmann, J.R. Westphal, E.T. Waas, A.J.W. Zendman, I.M.H.A. Cornelissen, D.J. Ruiter, G.N.P. van Muijen, Matrix metalloproteinases in human melanoma cell lines and xenografts: increased expression of activated matrix metalloproteinase-2 (MMP-2) correlates with melanoma progression, Br. J. Cancer 81 (1999) 774–782.
[12] J.H. Kim, T.H. Kim, J.W. Jang, Y.J. Jang, K.H. Lee, S.T. Lee, Analysis of matrix metalloproteinase mRNAs expressed in hepatocellular carcinoma cell lines, Mol. Cells 12 (2001) 32–40.
[13] Y. Murawaki, S. Yamada, Y. Ikuta, H. Kawasaki, Clinical usefulness of serum matrix metalloproteinase-2 concentration in patients with chronic viral liver disease, Hepatology 30 (1999) 1090–1098.
[14] S. Kawakami, C. Munakata, S. Fumoto, F. Yamashita, M. Hashida, Targeted delivery of prostaglandin E_1 to hepatocytes using galactosylated liposomes, J. Drug Target. 8 (2000) 137–142.
[15] Y. Hattori, S. Kawakami, F. Yamashita, M. Hashida, Controlled biodistribution of galactosylated liposomes and incorporated probucol in hepatocyte-selective drug targeting, J. Control. Release 69 (2000) 369–377.
[16] S. Kawakami, C. Munakata, S. Fumoto, F. Yamashita, M. Hashida, Novel galactosylated liposomes for hepatocyte-selective targeting of lipophilic drugs, J. Pharm. Sci. 90 (2001) 105–113.
[17] F. Kratz, J. Drevs, G. Bing, C. Stockmar, K. Scheuermann, P. Lazar, C. Unger, Development and in vitro efficacy of novel MMP-2 and MMP-9 specific doxorubicin albumin conjugates, Bioorg. Med. Chem. Lett. 11 (2001) 2001–2006.
[18] A.M. Mansour, J. Drevs, N. Esser, F.M. Hamada, O.A. Badary, C. Unger, I. Fichtner, F. Kratz, A new approach for the treatment of malignant melanoma: enhanced antitumor efficacy of an albumin-binding doxorubicin prodrug that is cleaved by matrix metalloproteinase 2, Cancer Res. 63 (2003) 4062–4026.
[19] C. Managit, S. Kawakami, M. Nishikawa, F. Yamashita, M. Hashida, Targeted and sustained drug delivery using PEGylated galactosylated liposomes, Int. J. Pharm. 266 (2003) 77–84.
[20] D. Papahadjopoulos, T.M. Allen, A. Gabizon, E. Mayhew, K. Matthay, S.K. Huang, K.D. Lee, M.C. Woodle, D.D. Lasic, C. Redemann, Sterically stabilized liposomes: improvements in pharmacokinetics and antitumor therapeutic efficacy, Proc. Natl. Acad. Sci. U. S. A. 88 (1991) 11460–11464.
[21] W. Zhao, H. Liu, S. Xu, F. Entschladen, B. Niggemann, K.S. Zanker, R. Han, Migration and metalloproteinases determine the invasive potential of mouse melanoma cells, but not melanin and telomerase, Cancer Lett. 162 (2001) S49–S55.
[22] R. Schwendener, H. Schott, Lipophilic arabinofuranosyl cytosine derivatives in leptosomes, Methods Enzymol. 391 (2005) 58–70.
[23] R.A. Schwendener, K. Friedl, H. Depenbrock, H. Schott, A.R. Hanauske, In vitro activity of liposomal *N*4octadecyl-1-β-L-arabinofuranosylcytosine (NOAC), a new lipophilic derivative of 1-β-D-arabinofuranocylcytosine on biopsized clonogenic human tumor cells and hematopoietic precursor cells, Invest. New Drugs 19 (2001) 203–210.
[24] S.K. Koller-Lucae, M.J. Suter, K.M. Rentsch, H. Schott, R.A. Schwendener, Metabolism of the new liposomal anticancer drug *N*4-octadecyl-1-β-D-arabinofuranosylcytosine in mice, Drug Metab. Dispos. 27 (1999) 342–350.
[25] Y.C. Lee, C.P. Stowell, M.J. Krantz, 2-Imino-2-methoxyethyl 1-thioglycosides: new reagents for attaching sugars to proteins, Biochemistry 15 (1976) 3956–3963.
[26] S. Kawakami, F. Yamashita, M. Nishikawa, Y. Takakura, M. Hashida, Asialoglycoprotein receptor-mediated gene transfer using novel galactosylated cationic liposomes, Biochem. Biophys. Res. Commun. 252 (1998) 78–83.
[27] R.M. Senior, G.L. Griffin, C.J. Fliszar, S.D. Shapiro, G.I. Goldberg, H.G. Welgus, Human 92- and 72-kilodalton type IV collagenases are elastases, J. Biol. Chem. 266 (1991) 7870–7875.
[28] A.F. Habeeb, Determination of free amino groups in proteins by trinitrobenzenesulfonic acid, Anal. Biochem. 14 (1966) 328–336.
[29] T. Takagi, M. Hashiguchi, R.I. Mahato, H. Tokuda, Y. Takakura, M. Hashida, Involvement of specific mechanism in plasmid DNA uptake by mouse peritoneal macrophages, Biochem. Biophys. Res. Commun. 245 (1998) 729–733.
[30] T. Mosmann, Rapid colorimetric assay for cellular growth and survival: application to proliferation and cytotoxicity assays, J. Immunol. Methods 65 (1983) 55–63.
[31] L.A. Kirkham, A.R. Bateman, A.A. Melcher, R.G. Vile, A.K. Fielding, Lack of specificity of cell-surface protease targeting of a cytotoxic hyperfusogenic gibbon ape leukaemia virus envelope glycoprotein, J. Gene Med. 4 (2002) 592–600.
[32] R.M. Schneider, Y. Medvedovska, I. Hartl, B. Voelker, M.P. Chadwick, S. J. Russell, K. Cichutek, C.J. Buchholz, Directed evolution of retroviruses activatable by tumour-associated matrix metalloproteases, Gene Ther. 10 (2003) 1370–1380.

[33] S. Chowdhury, K.A. Chester, J. Bridgewater, M.K. Collins, F. Martin, Efficient retroviral vector targeting of carcinoembryonic antigen-positive tumors, Mol. Ther. 9 (2004) 85–92.
[34] C.F. Albright, N. Graciani, W. Han, E. Yue, R. Stein, Z. Lai, M. Diamond, R. Dowling, L. Grimminger, S.Y. Zhang, D. Behrens, A. Musselman, R. Bruckner, M. Zhang, X. Jiang, D. Hu, A. Higley, S. Dimeo, M. Rafalski, S. Mandlekar, B. Car, S. Yeleswaram, A. Stern, R.A. Copeland, A. Combs, S.P. Seitz, G.L. Trainor, R. Taub, P. Huang, A. Oliff, Matrix metalloproteinase-activated doxorubicin prodrugs inhibit HT1080 xenograft growth better than doxorubicin with less toxicity, Mol. Cancer Ther. 4 (2005) 751–760.
[35] Y. Chau, R.F. Padera, N.M. Dang, R. Langer, Antitumor efficacy of a novel polymer-peptide-drug conjugate in human tumor xenograft models, Int. J. Cancer 118 (2006) 1519–1526.
[36] J.R. Tauro, R.A. Gemeinhart, Matrix metalloprotease triggered delivery of cancer chemotherapeutics from hydrogel matrixes, Bioconjug. Chem. 16 (2005) 1133–1139.
[37] H. Nagase, G.B. Fields, Human matrix metalloproteinase specificity studies using collagen sequence-based synthetic peptides, Biopolymers 40 (1996) 399–416.
[38] R.E. Galardy, D. Grobelny, H.G. Foellmer, L.A. Fernandez, Inhibition of angiogenesis by the matrix metalloprotease inhibitor *N*-[2R-2-(hydroxamidocarbonymethyl)-4-methylpentanoyl]]-L-tryptophan methylamide, Cancer Res. 54 (1994) 4715–4718.
[39] R. Ogata, T. Torimura, M. Kin, T. Ueno, Y. Tateishi, R. Kuromatsu, Y. Shimauchi, M. Sakamoto, S. Tamaki, M. Sata, K. Tanikawa, Increased expression of membrane type 1 matrix metalloproteinase and matrix metalloproteinase-2 with tumor dedifferentiation in hepatocellular carcinomas, Hum. Pathol. 30 (1999) 443–450.
[40] R.A. Schwendener, D.H. Horber, C. Ottiger, H. Schott, Preclinical properties of *N*4-hexadecyl- and *N*4-octadecyl-1-β-Darabinofuranosylcytosine in liposomal preparations, J. Liposome Res. 5 (1995) 27–47.
[41] M.E. Price, R.M. Cornelius, J.L. Brash, Protein adsorption to polyethylene glycol modified liposomes from fibrinogen solution and from plasma, Biochim. Biophys. Acta 1512 (2001) 191–205.
[42] Z. Xu, R.E. Marchant, Adsorption of plasma proteins on polyethylene oxide-modified lipid bilayers studied by total internal reflection fluorescence, Biomaterials 21 (2000) 1075–1083.
[43] S. Arii, M. Mise, T. Harada, M. Furutani, S. Ishigami, M. Niwano, M. Mizumoto, M. Fukumoto, M. Imamura, Hepatology 24 (1996) 316–322.
[44] B.E. Turk, L.L. Huang, E.T. Piro, L.C. Cantley, Determination of protease cleavage site motifs using mixture-based oriented peptide libraries, Nat. Biotechnol. 19 (2001) 661–667.
[45] A. Gabizon, H. Shmeeda, A.T. Horowitz, S. Zalipsky, Tumor cell targeting of liposome-entrapped drugs with phospholipid-anchored folic acid-PEG conjugates, Adv. Drug Deliv. Rev. 56 (2004) 1177–1192.
[46] K. Maruyama, O. Ishida, S. Kasaoka, T. Takizawa, N. Utoguchi, A. Shinohara, M. Chiba, H. Kobayashi, M. Eriguchi, H. Yanagie, Intracellular targeting of sodium mercaptoundecahydrododecaborate (BSH) to solid tumors by transferrin-PEG liposomes, for boron neutron-capture therapy (BNCT), J. Control. Release 98 (2004) 195–207.

THE JOURNAL OF GENE MEDICINE
J Gene Med 2006; 8: 824–834.
Published online 20 April 2006 in Wiley InterScience (www.interscience.wiley.com) **DOI:** 10.1002/jgm.910

RESEARCH ARTICLE

Enhanced DNA vaccine potency by mannosylated lipoplex after intraperitoneal administration

Yoshiyuki Hattori
Shigeru Kawakami
Yan Lu
Kazumi Nakamura
Fumiyoshi Yamashita
Mitsuru Hashida*

Department of Drug Delivery Research, Graduate School of Pharmaceutical Sciences, Kyoto University, Sakyo-ku, Kyoto 606-8501, Japan

*Correspondence to:
Mitsuru Hashida, Department of Drug Delivery Research, Graduate School of Pharmaceutical Sciences, Kyoto University, Sakyo-ku, Kyoto 606-8501, Japan. E-mail: hashidam@pharm.kyoto-u.ac.jp

Received: 15 December 2005
Revised: 31 January 2006
Accepted: 1 February 2006

Abstract

Background Here we describe a novel DNA vaccine formulation that can enhance cytotoxic T lymphocyte (CTL) activity through efficient gene delivery to dendritic cells (DCs) by mannose receptor-mediated endocytosis.

Methods Ovalbumin (OVA) was selected as a model antigen for vaccination; accordingly, OVA-encoding pDNA (pCMV-OVA) was constructed to evaluate DNA vaccination. Mannosylated cationic liposomes (Man-liposomes) were prepared using cholesten-5-yloxy-*N*-{4-[(1-imino-2-D-thiomannosylethyl)amino]butyl}formamide (Man-C4-Chol) with cationic lipid. The potency of the mannosylated liposome/pCMV-OVA complex (Man-lipoplex) was evaluated by measuring OVA mRNA in $CD11c^+$ cells, CTL activity, and the OVA-specific anti-tumor effect after *in vivo* administration.

Results An *in vitro* study using DC2.4 cells demonstrated that Man-liposomes could transfect pCMV-OVA more efficiently than cationic liposomes via mannose receptor-mediated endocytosis. *In vivo* studies revealed that the Man-lipoplex exhibited higher OVA mRNA expression in $CD11c^+$ cells in the spleen and peritoneal cavity and provided a stronger OVA-specific CTL response than intraperitoneal (i.p.) administration of the conventional lipoplex and intramuscular (i.m.) administration of naked pCMV-OVA, the standard protocol for DNA vaccination. Pre-immunization with the Man-lipoplex provided much better OVA-specific anti-tumor effect than naked pCMV-OVA via the i.m. route.

Conclusions These results suggested that *in vivo* active targeting of DNA vaccine to DCs with Man-lipoplex might prove useful for the rational design of DNA vaccine. Copyright © 2006 John Wiley & Sons, Ltd.

Keywords gene therapy; DNA vaccine; mannosylated liposomes; non-viral vectors

Introduction

DNA vaccine, plasmid DNA (pDNA)-encoding antigen from a pathogen, is of great interest in gene therapy as a means of immunotherapy against refractory diseases such as cancer and viral infections because the administration of naked pDNA-encoding antigen proteins induces not only an antibody response, but also a potent cytotoxic T lymphocyte (CTL) response in animal models [1–3]. Recent immunological studies have demonstrated that gene transfection and subsequent activation of antigen-presenting cells (APCs), dendritic cells (DCs) and macrophages are important for efficient DNA

vaccine therapy [4–6]. Although some clinical trials involving melanoma, human imuunodeficiency virus, and HCV have been performed using topical administration of naked pDNA [7–9], the results are not good enough for clinical therapy. In order to overcome this problem, it is important to develop gene delivery carriers for *in vivo* APC-selective gene transfection.

In spite of the high transfection efficiency of viral vectors, they still need to be improved from the point of view of safety issues [10–12]. The use of non-viral vectors is one of the possible approaches for *in vivo* gene delivery because they are free from some of the risks inherent in these systems. Furthermore, the characteristics of non-viral vectors can be more easily modified than those of viral vectors. To achieve targeted gene delivery, a number of receptor-mediated gene delivery systems have been developed [13–16] including our carriers [17–22]. As far as *in vivo* selective gene delivery to APCs is concerned, mannose has been shown to be a promising ligand to target APCs because these cells have a large number of mannose receptors.

Recently, we have developed several types of macromolecular [18] and particulate [22,23] gene carriers for macrophage-selective gene transfection *in vivo*. Among them, cationic liposomes containing cholesten-5-yloxy-*N*-{4-[(1-imino-2-D-thiomannosylethyl)amino]butyl} formamide (Man-C4-Chol) are some of the most interesting potential gene transfection carriers [22,23] that can be efficiently recognized by mannose receptors on macrophages in liver. Man-C4-Chol exhibits bifunctional properties, i.e., an imino group for binding to pDNA via electrostatic interaction and a mannose residue for the cell-surface receptors in APCs [22]. Therefore, a high density of mannose residues can be provided on the liposome surface without affecting the binding of the cationic liposomes to pDNA. More recently, we have demonstrated that intravenously administrated pCMV-OVA complexed with mannosylated liposomes (Man-lipoplex) enhances MHC class I antigen presentation, but no measurable CTL response was observed [24], suggesting that not only cell-selective gene transfection but also enhanced transfection efficiency in DCs is needed for gene therapy.

Intraperitoneal (i.p.) administration has some advantages as far as the transfection efficacy to DCs by Man-lipoplex is concerned; this is because of (i) high accessibility to APCs in the peritoneal cavity and lymph nodes, (ii) long retention of the lipoplex, (iii) the presence of few biocomponents that reduce transfection activity, and (iv) the high capacity of the lipoplex solution. Taking these factors into consideration, i.p. administrated Man-lipoplex would enhance gene expression in APCs resulting in efficient DNA vaccine therapy. However, few reports are available on the effect of i.p. administered Man-lipoplex on DNA vaccine therapy.

The objective of this paper was to clarify the DNA vaccine potency after i.p. administration of Man-lipoplex. In the present study, ovalbumin (OVA)-encoding pDNA (pCMV-OVA) was selected as a model DNA vaccine. Using *in vitro* and *in vivo* experiments, the transfection efficacy to APCs was evaluated by measuring the OVA mRNA using quantitative reverse-transcription polymerase chain reaction (RT-PCR). After immunizing with Man-lipoplex, OVA-specific CTL responses and its antitumor effects against inoculated E.G7-OVA cells (OVA expressing cells), and its parental cell line, EL4 cells (OVA non-expressing cells), were also evaluated. The results obtained were compared with those of conventional lipoplex and naked pCMV-OVA.

Materials and methods

Materials

Cholesteryl chloroformate, HEPES, concanavalin A, G418, and immunogloblin G were obtained from Sigma Chemicals Inc. (St. Louis, MO, USA). *N*-[1-(2,3-Dioleyloxy)propyl]-*N*,*N*,*N*-trimethylammonium chloride (DOTMA) and *N*-(4-aminobutyl)carbamic acid *tert*-butyl ester were obtained from Tokyo Chemical Industry Co. (Tokyo, Japan). Dioleoylphosphatidylethanolamine (DOPE) was purchased from Avanti Polar Lipids, Inc. (Alabaster, AL, USA). pVAX I, fetal bovine serum (FBS), and Opti-MEM I® were obtained from Invitrogen Co. (Carlsbad, CA, USA). Anti-CD11c monoclonal antibody (N418)-labeled magnetic beads were purchased from Miltenyi Biotec Inc. (Auburn, CA, USA). Nucleic acid purification kit magextractor®-RNA was purchased from Toyobo Co., Ltd. (Osaka, Japan). The first strand cDNA synthesis kit for RT-PCR, Lightcycler™ faststart DNA master hybridization probes, and a Lightcycler™-Primer/Probes set for mouse β-actin were purchased from Roche Diagnostics Co. (Indianapolis, IN, USA). Primers/probes for OVA were purchased from Nihon Gene Research Labs Inc. (Miyagi, Japan). All other chemicals were of the highest purity available.

Animals

Female ICR mice (4–5 weeks old) and C57BL/6 mice (6–8 weeks old) were purchased from the Shizuoka Agricultural Cooperative Association for Laboratory Animals (Shizuoka, Japan). All animal experiments were carried out in accordance with the Principles of Laboratory Animal Care as adopted and promulgated by the US National Institutes of Health and the guideline for animal experiments of Kyoto University.

Cell line

DC2.4 cells, a cell line of murine dendritic cells (DCs, haplotype H-2b) [25], were kindly provided by Dr. K. L. Rock (University of Massachusetts Medical School, Worcester, MA, USA). The expression of mannose receptors in this cell line has been confirmed elsewhere [26]. Therefore, DC2.4 cells are a suitable model of DCs.

EL4 cells (ATCC: TIB-39) and E.G7-OVA cells (ATCC: CRL-2113) were purchased from the American Type Culture Collection (ATCC, Manassas, VA, USA) and maintained in Dulbecco's modified Eagle's medium supplemented with 10% FBS and RPMI 1640 supplemented with 10% FBS, 4.5 g/l glucose, 10 mM HEPES, 1 mM sodium pyruvate, 0.05 mM 2-mercaptoethanol and 0.4 mg/ml G418.

Synthesis of Man-C4-Chol and Gal-C4-Chol

Man-C4-Chol and Gal-C4-Chol were synthesized as described previously [19,22]. Briefly, *N*-(4-aminobutyl)-(cholesten-5-yloxyl)formamide (C4-Chol) was synthesized from cholesteryl chloroformate and *N*-(4-aminobutyl)carbamic acid *tert*-butyl ester. The C4-Chol was reacted with 5 equivalents of 2-imino-2-methoxyethyl-1-thiomannoside or 2-imino-2-methoxyethyl-1-thiogalactoside [27] in pyridine containing 1.1 equivalents of triethylamine for 24 h. After evaporation of the reaction mixture *in vacuo*, the resultant material was suspended in water and dialyzed against water for 48 h, and then lyophilized.

Construction and preparation of pCMV-OVA

pCMV-OVA was constructed by subcloning the EcoRI chicken egg albumin (ovalbumin) cDNA fragment from pAc-neo-OVA [28], which was kindly provided by Dr. M. J. Bevan (University of Washington, Seattle, WA, USA), into the polylinker of pVAX I. pCMV-OVA was amplified in the *E. coli* strain, DH5α, then isolated, and purified using a Qiagen plasmid giga kit (Qiagen GmbH, Hilden, Germany). The endotoxin in pCMV-OVA solution was removed by the Triton X-114 method.

Preparation of cationic liposomes

Liposomes were prepared using the method reported previously [19,22]. Briefly, DOTMA, Chol, and Man-C4-Chol or Gal-C4-Chol were mixed in chloroform at a molar ratio of 2:1:1:0, 2:1:0:1, and 2:2:0:0 to prepare Man-liposomes, Gal-liposomes, and cationic liposomes, respectively. Then, the mixture was dried, vacuum desiccated, and resuspended in sterile 20 mM HEPES buffer (pH 7.8) or 5% dextrose solution in a sterile test tube for *in vitro* and *in vivo* experiments, respectively. After hydration, the dispersion was sonicated for 5 min in a bath sonicator to produce liposomes and then sterilized by passing through a 0.45 μm filter (Nihon-Millipore Ltd., Tokyo, Japan).

Preparation of lipoplex for *in vitro* study

Lipoplex was prepared using the method reported previously [19,22]. Briefly, equal volumes of pCMV-OVA and stock liposome solution were diluted with Opti-MEM I® in 15 ml Falcon tubes. Then, pCMV-OVA solution was added rapidly to the surface of the liposome solution at a charge ratio (−/+) of 1.0:2.3 using a micropipette (Pipetman®, Gilson, Villier-le Bel, France) and the mixture was agitated rapidly by pumping it up and down twice in the pipette tip.

Preparation of lipoplex for *in vivo* study

All cationic liposome/pCMV-OVA complexes for *in vivo* experiments were prepared under the optimal conditions for cell-selective gene transfection as reported previously [29–31]. Briefly, equal volumes of pCMV-OVA and stock liposome solution were diluted with 5% dextrose in 15 ml tubes. Then, pCMV-OVA solution was added rapidly to the surface of the liposome solution using a micropipette and the mixture was agitated rapidly by pumping it up and down twice in the pipette tip. The mean particle sizes were measured by dynamic light scattering spectrophotometry (LS-900; Otsuka Electronics Co., Ltd., Osaka, Japan). The zeta-potential of the lipoplexes was measured by the laser-Doppler electrophoresis method with a Zetasizer Nano ZS (Malvern Instruments Ltd., Worcestershire, UK).

Uptake characteristics by DC2.4 cells

Uptake study was performed by the method reported previously [19,22]. Briefly, the DC2.4 cells were plated on a 24-well plate at a density of 0.65×10^5 cells/cm^2 and cultivated in 500 μl RPMI supplemented with 10% FBS. Twenty-four hours later, the culture medium was replaced with an equivalent volume of Hanks medium (Nissui Pharmaceutical Co., Ltd., Tokyo, Japan) containing 1 kBq/ml [^{32}P]-pCMV-OVA, 0.5 mg/ml cold pCMV-OVA and cationic liposomes at a charge ratio (−/+) of 1.0:2.3. After incubation for given time periods, the solution was quickly removed by aspiration, the cells were washed five times with ice-cold HBSS buffer and then solubilized in 0.3 M NaOH solution with 10% Triton X-100 (0.3 ml). The radioactivity was measured by liquid scintillation counting (LSC-500; Beckman, Inc., Tokyo, Japan) and the protein content was determined by a modification of the Lowry method. The effect of the presence of 0.125 mg/ml mannan was determined in the same system.

Transfection activity by DC2.4 cells

DC2.4 cells were seeded in 10.5 cm^2 dishes at a density of 0.65×10^5 cells/cm^2 in RPMI 1640 medium supplemented with 10% FBS. After 24 h in culture, the culture medium was replaced with Opti-MEM I® containing 0.5 μg/ml pCMV-OVA and cationic liposomes. Six hours later, the incubation medium was replaced again with RPMI 1640 supplemented with 10% FBS and incubated for an additional 6 h. Then, the cells were

scraped and suspended in 200 µl pH 7.4 phosphate-buffered saline (PBS). Total RNA was isolated from DC2.4 cells with MagExtractor MFX-2000 (Toyobo Co., Ltd., Osaka, Japan) and MagExtractor-RNA following the manufacturer's instructions. Reverse transcription of mRNA was carried out using a first strand cDNA synthesis kit as follows: total RNA was added to the oligo dT primer (0.8 µg/µl) solution, and incubated at 42 °C for 60 min with a program temperature control system PC-808 (Astec Co., Ltd., Fukuoka, Japan). Real-time PCR was performed using the Lightcycler™ quick system 350S (Roche Diagnostics Co., Indianapolis, IN, USA) with hybridization probes. Primer and hybridization probes for OVA cDNA were constructed as follows: primer, 5′-GCGTCTCTGAATTTAGGG-3′ (forward) and 5′-TACCCCTGATACTACAGTGC-3′ (reverse); hybridization probes, 5′-CTTCTGTATCAAGCACATCGCAACCAACG-3′-fluorescein isothiocyanate (FITC) and Lightcycler™-Red640 (LCRed)-5′-CGTTCTCTTCTTTGGCAGATGTGT-TTCCCC-3′. The PCR reaction for detection of the OVA gene was carried out in a final volume of 20 µl containing: (i) 2 µl DNA Master hybridization probes 10× (DNA Master hybridization probes kit); (ii) 1.6 µl 25 mM $MgCl_2$; (iii) 1.5 µl forward and reverse primers (final concentration 0.75 µM); (iv) 1 µl 2 µM FITC-labeled hybridization probes and 2 µl 2 µM LCRed-labeled probes (final concentrations 0.2 and 0.4 µM, respectively); (v) 5.4 µl H_2O; (vi) 5 ml cDNA or pCMV-OVA solution. For the mouse β-actin cDNA measurements, samples were prepared in accordance with the instruction manuals. After an initial denaturation step at 95 °C for 10 min, temperature cycling was initiated. Each cycle consisted of denaturation at 95 °C for 10 s, hybridization at 60 °C for 15 s, and elongation at 72 °C for 10 s. The fluorescent signal was acquired at the end of the hybridization step (F2/F1 channels). The total number of cycles performed was 40. The mRNA copy numbers were calculated for each sample from the standard curve using the instrument software ('Arithmetic Fit Point analysis' for the Lightcycler). Results were expressed as relative copy numbers calculated relative to β-actin mRNA (copy number of OVA mRNA/copy number of β-actin mRNA).

Quantification of OVA mRNA in CD11c$^+$ cells after i.p. administration by quantitative PCR

pCMV-OVA (100 µg) or lipoplex was injected via the i.p. route. Spleens and peritoneal cells were harvested 6 h after i.p. administration and single cell suspensions of spleen cells were prepared in ice-cold RPMI 1640 medium. Ice-cold RPMI 1640 medium (5 ml) was injected and then peritoneal cells were collected as a cell suspension in RPMI medium. Following this, red blood cells were removed by incubation with Tris-NH_4Cl solution for 10 min at room temperature. Positive selection of CD11c$^+$ cells was carried out by magnetic cell sorting with auto MACS (Miltenyi Biotec Inc., Auburn, CA, USA) following the manufacturer's instructions. Briefly, the cell suspension was incubated with PBS containing 1 mg/ml IgG to block the Fcγ receptors of macrophages. Then, CD11c$^+$ cells were labeled by incubating with anti-CD11c monoclonal antibody (N418)-labeled magnetic beads. After washing three times, CD11c$^+$ cells were collected by auto MACS. Total RNA was isolated from the recovered CD11c$^+$ cells with a MagExtractor MFX-2000 (Toyobo Co., Ltd., Osaka, Japan) and MagExtractor-RNA following the manufacturer's instructions. Reverse transcription and quantitative PCR of OVA and β-actin mRNA were performed as described in the section 'Transfection activity by DC2.4 cells'.

Induction of OVA-specific CTL

C57BL/6 mice were immunized with naked pCMV-OVA (50 or 100 µg) or lipoplexes by i.p., i.m., or intradermal (i.d.) administration three times at intervals of 2 weeks. Two weeks after the last immunization, the spleens of each group were harvested and a single cell suspension was prepared in ice-cold RPMI 1640 medium. Then, the spleen cells were resuspended in RPMI 1640 medium supplemented with 10% FBS and 2-mercaptoethanol. The recovered spleen cells were plated in a 25-cm flask at 5×10^6 cells/ml along with MMC and E.G7-OVA cells and treated for 1 h (100 µg/ml, 1 h). Four days after cultivation, non-adherent cells were harvested, washed, and plated with relevant or irrelevant target cells at effector/target (E/T) ratios of 100 : 1, 50 : 1, 25 : 1, and 12.5 : 1. The target cells were E.G7-OVA cells or their parental cell line, EL4 cells. The target cell (E.G7-OVA or EL4 cells) suspensions in RPMI medium (2.5×10^7 cells/ml) were incubated with ^{51}Cr (7.4 MBq/ml) for 1 h. Following incubation, the cells were washed five times and then resuspended at 2×10^5 cells/ml. The target cells (E.G7-OVA or EL4 cells; 2×10^4 cells) were added to each well of a 96-well microtiter plate, along with 2×10^6, 1×10^6, 5×10^5, or 2.5×10^5 spleen cells and the plates were mixed and incubated for 4 h at 37 °C and 5% CO_2 in an incubator. After further centrifugation, 100 µl supernatant was collected from each well and the radioactivity released was measured in a gamma counter. The percentage ^{51}Cr release was calculated as follows: specific lysis (%) = [(experimental ^{51}Cr release − spontaneous ^{51}Cr release)/(maximum ^{51}Cr release − spontaneous ^{51}Cr release)] × 100). The percentage OVA-specific ^{51}Cr release was calculated as (% of ^{51}Cr release from E.G7-OVA) − (% of ^{51}Cr release from EL4).

Evaluation of protection against transplanted tumor cells in mice

C57BL/6 mice were immunized three times by i.p. or i.m. administration of naked pCMV-OVA (100 µg) or lipoplex at 2-week intervals. Then 2 weeks after the last